

DOE/ER--0451P

DE90 010157

*Prepared for:*

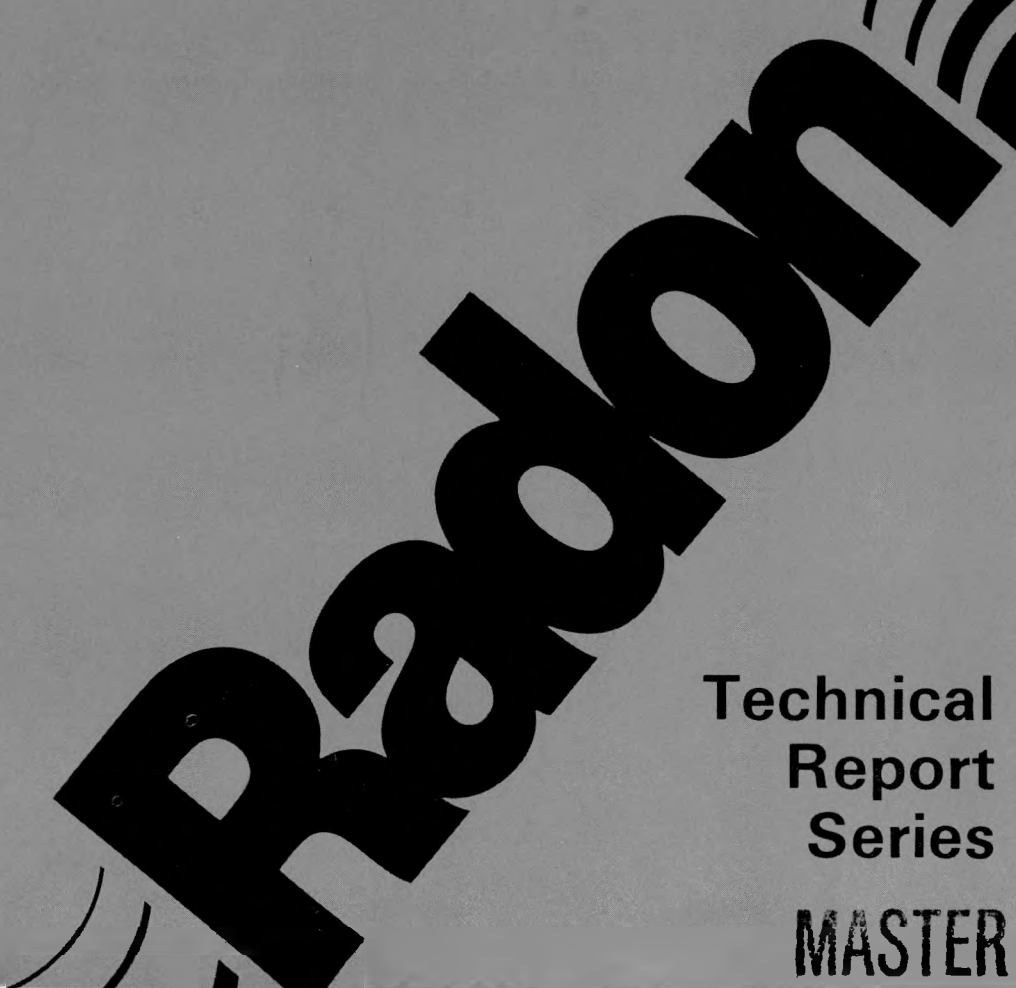
U.S. Department of Energy  
Office of Energy Research  
Office of Health and Environmental Research  
Washington, D.C. 20545  
*Prepared Under DOE Contract*  
No. DE-FG02-89ER60878

*By:*

Philip K. Hopke  
Department of Chemistry  
Clarkson University  
Potsdam, N.Y. 13676

# **A Critical Review of Measurements of the "Unattached" Fraction of Radon Decay Products**

January 1990



**radon**

**Technical  
Report  
Series**

**MASTER**

DISTRIBUTION OF THIS DOCUMENT IS UNLIMITED

## **DISCLAIMER**

**This report was prepared as an account of work sponsored by an agency of the United States Government. Neither the United States Government nor any agency thereof, nor any of their employees, makes any warranty, express or implied, or assumes any legal liability or responsibility for the accuracy, completeness, or usefulness of any information, apparatus, product, or process disclosed, or represents that its use would not infringe privately owned rights. Reference herein to any specific commercial product, process, or service by trade name, trademark, manufacturer, or otherwise does not necessarily constitute or imply its endorsement, recommendation, or favoring by the United States Government or any agency thereof. The views and opinions of authors expressed herein do not necessarily state or reflect those of the United States Government or any agency thereof.**

---

## **DISCLAIMER**

**Portions of this document may be illegible in electronic image products. Images are produced from the best available original document.**

## Preface

"A Critical Review of Measurements of the Unattached Fraction of Radon Decay Products," by Dr. Philip Hopke, is another in the technical reports series from the Department of Energy, Office of Health and Environmental Research (OHER) Radon Research Program. This report, as in all the technical reports, provides state-of-the-art scientific knowledge in one of the many disciplines currently being funded to understand the complex issues regarding indoor radon.

Dr Philip Hopke, a major contributor both to the understanding of the complex behavior of radon decay products and to the OHER Radon Program, has written a review of the literature and measurements of the "unattached" fraction of radon progeny. In light of the importance of this fraction to estimates of dose received by the critical cells in the lung, this volume is both significant and timely. It will provide the reader with all the pertinent literature and measurements, as well as an explanation for their significance.

Several other types of publications complete the OHER radon publication effort. These include an annual program report, summary reviews of selected scientific areas, critical bibliographies, and a quarterly research notes publication.

Information on the Radon Research Program or the radon publications may be obtained from:

Susan L. Rose, Ph.D.  
Radon Program Manager  
Office of Health and Environmental  
Research, ER-73  
Department of Energy, GTN  
Washington, D.C. 20545

## Abstract

Exposure to radon and its decay products is known to cause lung cancer. It is the deposition of the decay products within the respiratory tract that delivers the dose leading to adverse health effects. An important concept in understanding the health effects of the radon progeny is the "unattached" fraction. It was suggested that there is a highly diffusive form of the radon and thoron decay products that can be fully deposited in the respiratory system. This smallest fraction of the size distribution has been referred to as the "unattached fraction." Recent evidence suggests that the "unattached" decay product atoms are associated with ultrafine particles (0.5 to 5 nm in diameter). However, there is a long history of this operationally defined "unattached" fraction in the radon literature and the "unattached" fraction has been given extra importance in estimating the health effects of radon decay products.

Initial measurements were made using diffusional deposition in tubes to separate the high diffusivity "unattached" activity from that associated with lower diffusion coefficient particles. Subsequently, wire screens were used to estimate "unattached" Rn daughter fractions in ambient and mine atmospheres. Wire screen penetration theory along with a semi-empirically corrected diffusion coefficient equation can be used to characterize the previously reported "unattached" fraction measurements. Collection efficiency curves have been estimated for previously published wire screen "unattached" fraction measurements and the measurements available in the literature are reviewed and discussed. Although the measurement methods have been available for many years, only limited measurements are available for either mine or indoor atmospheres.

If the "unattached" fraction is in reality an ultrafine cluster mode in the 0.5-5 nm size range, the collection efficiency versus particle diameter characteristics of wire screens do not permit a distinct separation of the "unattached" and "attached" fractions. Thus, "unattached" fraction measurements cannot provide the detailed information that is needed for more accurate dosimetric calculations. The better understanding of screen penetration has permitted the development of new systems that can measure the activity-weighted size distributions over the full range of interest (0.5 to 500 nm). There have only been limited measurements made since the development of these graded screen array systems. The available data are presented.

Finally, the purpose for measuring unattached fraction is to estimate the dose to the respiratory tract arising from the deposition of radon decay products to which the individual is exposed. Therefore, if measurements could be made in a manner that better reflected the aerodynamic behavior of the radon progeny in the respiratory tract, then the assessment of exposure could be directly related to dose with far greater accuracy than has been previously possible. Respiratory deposition models can serve as basis for such a system and the design concepts of such a measurement system is presented.

## TABLE OF CONTENTS

Abstract .....	i
TABLE OF CONTENTS .....	ii
LIST OF TABLES .....	iii
LIST OF FIGURES .....	iv
INTRODUCTION AND BACKGROUND .....	1
RELATIONSHIP BETWEEN PARTICLE SIZE AND DIFFUSION COEFFICIENT .....	3
PENETRATION OF AEROSOLS THROUGH A TUBE .....	5
DEPOSITION OF ULTRAFINE PARTICLES ONTO WIRE SCREENS .....	6
REVIEW OF PAST "UNATTACHED" FRACTION MEASUREMENTS .....	8
<u>Diffusion Sampler Measurements</u> .....	8
INTRODUCTION .....	8
MINE ATMOSPHERES .....	9
AMBIENT AND INDOOR ATMOSPHERES .....	24
<u>Wire Screen Measurements</u> .....	14
INTRODUCTION .....	14
MINE ATMOSPHERES .....	19
AMBIENT AND INDOOR ATMOSPHERES .....	24
<u>Conclusions</u> .....	31
ACTIVITY-WEIGHTED SIZE DISTRIBUTIONS .....	34
SAMPLER DESIGN BASED ON RESPIRATORY DEPOSITION .....	46
<u>Introduction</u> .....	46
<u>Nasal Deposition</u> .....	46
<u>Bronchial Deposition</u> .....	48
<u>Sampler Design</u> .....	50
REVIEW AND RECOMMENDATIONS .....	51
REFERENCES .....	57

## LIST OF TABLES

Table 1.	Wire screen parameters and face velocities used in published wire screen "unattached" fraction measurements. Underestimation of "unattached" fraction is based on a log-normally distributed mode with $d_m=1.0$ nm and $\sigma_g=1.5$ . . . . .	16
Table 2.	"Unattached" fraction measurements reported by Bigu and Kirk (1980). . . . .	23
Table 3.	Values for the mean and median "unattached" fractions as measured in a Norwegian iron ore mine by Stranden and Berteig (1982). . . . .	24
Table 4.	Concentrations of radon, "attached" and "unattached" activities, $f_p$ , F-values and particles measured in the ambient atmosphere near Göttingen (1 m above the ground during daylight) by Reineking and Porstendorfer (1990). . . . .	26
Table 5.	Summary results of the "unattached" fractions measured in a single Japanese house (Kojima and Abe, 1988). . . . .	33
Table 6.	Summary of activity size measurements made by Strong (1988) in two houses in the United Kingdom. . . . .	39
Table 7.	Assessment of measured screen penetration compared to theoretical predictions of Ingham (1975). . . . .	42

## LIST OF FIGURES

Figure 1.	Diffusion coefficient for particles 0.5-10 nm in diameter, plotted using the uncorrected and corrected Einstein - Cunningham equations, and the kinetic theory equation without the mass factor, $[(M+m)/M]^{1/2}$ . . . . .	5
Figure 2.	Assessment of penetration of radioactive particles into a cylindrical tube compared to the theoretical predictions of Ingham (1975). . . . .	7
Figure 3.	Fractional penetration through various mesh screens at a face velocity of 10 cm s <sup>-1</sup> . . . . .	9
Figure 4.	Collection efficiency of the HASL diffusion samplers as a function of flow rate redrawn from data in George and Hinchliffe (1972). The lines are simple first order regression lines drawn through each set of points. . . . .	11
Figure 5.	"Unattached" fraction of <sup>218</sup> Po as defined by ICRP (1959) measured in New Mexico uranium mines as a function of particle concentration. Data for this plot was taken from George and Hinchliffe (1972) and George <i>et al.</i> (1977). . . . .	11
Figure 6.	"Unattached" fraction of <sup>218</sup> Po as defined relative to total <sup>218</sup> Po measured in New Mexico uranium mines as a function of particle concentration. Data for this plot was taken from George and Hinchliffe (1972) and George <i>et al.</i> (1977). . . . .	12
Figure 7.	"Unattached" fraction measurements of Cooper <i>et al.</i> (1973). All of the results are the fraction of <sup>218</sup> Po activity that is "unattached." . . . . .	12
Figure 8.	Calculated penetration values for the Duggan and Howell (1969) diffusion battery. Open circles represent the initial calculation. Filled points are for a recalculation made to include the measured non-uniformity of inlet airflow. . . . .	13
Figure 9.	Comparison of Thomas-Hinchliffe empirical calibration and Yeh-Cheng screen penetration for a 120 mesh at a face velocity of 10 cm s <sup>-1</sup> . . . . .	15
Figure 10.	Collection characteristics for the wire mesh screen systems used in a number of the reported "unattached" fraction measurements. . . . .	17
Figure 11.	Collection efficiency curves for "typical" wire screens characterized by $d_p(50\%)$ values of 1, 2, 3, and 4 nm and presentation of a log-normal size distribution characteristic of the "unattached" fraction. . . . .	17
Figure 12.	Cumulative collection fraction of an ultrafine activity mode having a median diameter of 1.0 nm and geometric standard deviation of 1.5 for various wire screen systems characterized by their $d_p(50\%)$ values. . . . .	18

Figure 13.	"Unattached" fraction measurements of Raghavayya and Jones (1974) as corrected by Mercer (1975) as a function of particle concentration. . . . .	20
Figure 14.	Total "unattached" fraction, $f_u$ , as measured by Raghavayya and Jones (1974) with corrected values of Kotrappa and Mayya (1976). . . . .	21
Figure 15.	Equilibrium fraction calculated from the data of Raghavayya and Jones (1974) as corrected by Kotrappa and Mayya (1976) as a function of the condensation nuclei count. . . . .	22
Figure 16.	Distributions of the "unattached" fractions of the three radon decay products and PAEC measured in an iron ore mine. Redrawn from the graph in Stranden and Berteig (1982). . . . .	25
Figure 17.	"Unattached" fraction of potential alpha energy concentration, $f_p$ , as a function of the condensation nuclei concentration. Data taken from Porstendorfer (1987). . . . .	27
Figure 18.	Equilibrium factor as a function of condensation nuclei concentration. Data taken from Porstendorfer (1987). . . . .	27
Figure 19.	Time sequence of measurements in a Belgian house. Figure taken from Vanmarcke <i>et al.</i> (1985) and used with permission. . . . .	28
Figure 20.	Equilibrium factor and the "unattached" fraction of potential alpha energy concentration as a function of the estimated attachment rate based on measured aerosol size distributions. . . . .	28
Figure 21.	Radon and radon decay product concentrations measured during the Gent-Göttingen intercomparison study. Filled symbols are Gent; Open symbols are Göttingen. Figure taken from Vanmarcke <i>et al.</i> (1988) and used with permission. . . . .	29
Figure 22.	Evolution of the "unattached" and equilibrium fractions as measured in the Gent-Göttingen intercomparison study. Figure taken from Vanmarcke <i>et al.</i> (1988) and used with permission. . . . .	30
Figure 23.	Diurnal variation of the "unattached" fractions of each of the radon decay products and the aerosol concentration. Figure taken from Kojima and Abe (1988) and used with permission. . . . .	32
Figure 24.	Activity-weighted size distribution of the indoor aerosol in a closed room without additional aerosol sources. Figure taken from Reineking and Porstendorfer (1986) and used with permission. . . . .	36

Figure 25.	Activity-weighted size distribution of the indoor aerosol in a closed room with an additional aerosol source. Figure taken from Reineking and Porstendörfer (1986) and used with permission. . . . .	36
Figure 26.	$^{218}\text{Po}$ -weighted size distributions measured in house I. 1. cooking (5 min.); 2. frying food; 3. cooking soup; 4. cigarette smoldering. Figure taken from Tu and Knutson (1988a) and used with permission. . . . .	37
Figure 27.	$^{218}\text{Po}$ -weighted size distributions measured in house II after a kerosene heater was burned for: 1. 0 min; 2. 80 min; 3. 200 min. Figure taken from Tu and Knutson (1988a) and used with permission. . . . .	38
Figure 28.	Activity size distributions measured in a rural house kitchen by Strong (1988). Used with permission. . . . .	40
Figure 29.	Tri-modal activity size distribution measured by Strong (1989) under conditions of a) $F=0.36$ , $\text{CN}=10,000 \text{ cm}^{-3}$ ; b) $F=0.26$ , $\text{CN}=5000 \text{ cm}^{-3}$ . . . . .	41
Figure 30.	Typical Po-218, Pb-214, and Bi-214 activity size distributions observed in a house basement in Princeton, N.J. . . . .	43
Figure 31.	Po-218, Pb-214, and Bi-214 activity size distributions measured under typical conditions in the kitchen of the test house. . . . .	44
Figure 32.	Po-218, Pb-214, and Bi-214 activity size distributions measured during the continuous generation of aerosols from the kitchen gas stove burners. . . . .	45
Figure 33.	Fractional collection of particles in the nasal cavity as modeled by Equation 17. . . . .	48
Figure 34.	Fractional tracheobronchial deposition (generations 1-16) at $30 \text{ l min}^{-1}$ . Also shown is the collection characteristic of four 400 mesh screens at a face velocity of $12.0 \text{ cm s}^{-1}$ . . . . .	49

## INTRODUCTION AND BACKGROUND

Recent awareness of the health risks posed to the public by the inhalation and subsequent lung deposition of Rn decay products has resulted in a renewed interest in the properties of Rn and its progeny. The decay products rather than radon itself are the active species responsible for the health hazard because of their deposition in the respiratory tract followed by the release of ionizing radiation during their subsequent decay. The radon concentrations as well as the prolonged exposure periods related with indoor habitation make indoor radon a potential health hazard. The National Council on Radiological Protection (NCRP, 1984) estimated that 5,000-20,000 lung cancer deaths per year in the United States may be a result of prolonged indoor radon exposure (EPA, 1986). Currently Environmental Protection Agency uses an estimate of 20,000 deaths annually from radon-induced lung cancer in the general population (EPA, 1989). The "new" estimate was obtained by using revised risk coefficients from the underground miner studies of both the International Commission on Radiological Protection Report No. 50 (ICRP, 1987) and National Research Council's Panel on the Biological Effects of Ionizing Radiation risk estimates (BEIR IV, 1988).

Two important physical parameters in all lung dosimetry models used to estimate radiation doses from inhaled Rn decay products are the activity median diameter of the "attached" radioactive aerosol and the "unattached" fraction of  $^{218}\text{Po}$  (RaA) (James *et al.*, 1980; Jacobi and Eisfeld (1980); Harley and Pasternack, 1982). Traditionally defined, the "unattached" fraction constitutes free molecular daughter atoms or ions possibly clustered with other molecules such as  $\text{H}_2\text{O}$  as distinct from daughter atoms "attached" to particles in the preexisting ambient aerosol.

The measurement of the "unattached" fraction of Rn progeny has been the subject of extensive research. Diffusion, impaction, and electrostatic deposition methods have been employed for the separation of the "attached" and "unattached" fractions of radioactive aerosols in ambient and mine atmospheres (Van der Vooren *et al.*, 1982). However, from the recent studies of the neutralization rate for  $^{218}\text{Po}^+$  ions (Chu and Hopke, 1988), it is clear that most of the ions will be rapidly neutralized in the atmosphere and electrostatic collection will underestimate the "unattached" fraction. Jonassen (1984) and Jonassen and McLaughlin (1985) found that only about 10% of the "unattached" fraction as measured using a wire screen system was charged. Thus, the measurements of Blanc *et al.* (1968) and Chapuis *et al.* (1970) find

extremely small "unattached" fractions when actually what they have measured is that fraction of the highly diffusive daughter activity that is still charged. These results are in good agreement with later measurements of Jonassen and McLaughlin (1985). Thus, electrostatic measurements of "unattached" fractions will not be considered further in this report.

The studies based on diffusional collection of the "unattached" activity are characterized by their common use of a single, constant diffusion coefficient for "unattached"  $^{218}\text{Po}$ , originating from the first estimate of  $0.054 \text{ cm}^2\text{s}^{-1}$  for the diffusion coefficient of  $^{218}\text{Po}$  (Chamberlain and Dyson, 1956). Recent investigations have indicated that the "unattached"  $^{218}\text{Po}$  fraction is actually an ultrafine particle or cluster mode, 0.5-3 nm in diameter, rather than free molecular  $^{218}\text{Po}$  (Reineking and Porstendorfer, 1976). Busigin *et al.* (1981a) were the first to conclude that the diffusion coefficient of "unattached"  $^{218}\text{Po}$  in air could not be adequately described by a single number, given the experimentally observed range of  $0.005\text{-}0.1 \text{ cm}^2 \text{ s}^{-1}$ . Goldstein and Hopke (1985) have also shown experimentally that the diffusion coefficient for  $^{218}\text{Po}$  can be adjusted in the range  $0.03\text{-}0.08 \text{ cm}^2 \text{ s}^{-1}$  by controlling the admixed trace gases. Raes (1985) has applied classical nucleation theory to describe the growth of clusters in atmospheres containing  $^{218}\text{Po}$ ,  $\text{H}_2\text{O}$  and  $\text{SO}_2$ . The results of these studies strongly suggest that the so-called "unattached" fraction is actually an ultrafine particle mode in the 0.5-3.0 nm size range whose nature is dependent upon the gaseous environment surrounding the Rn decay products.

The detection of these ultrafine clusters by conventional particle detection devices such as condensation nuclei counters (CNCs) is precluded by the lack of sensitivity of these devices below particle diameters of 4 nm (Agarwal and Sem, 1980; Bartz *et al.*, 1985). However, the existence of the ultrafine cluster mode (0.5-3 nm diameter) in the activity size distribution has been observed in recent investigations by Reineking and Porstendorfer (1986) and by Tu and Knutson (1988a), using specially developed wire screen diffusion batteries. Wire screens, calibrated using a single, constant value for the  $^{218}\text{Po}$  diffusion coefficient and sampling an "unattached" fraction consisting of an ultrafine cluster mode in the activity size distribution would thus be unable to separate the "unattached" and the "attached" fractions.

Most of the initial "unattached" fraction measurements were made using the penetration of activity through a diffusion tube or diffusion battery to separate the highly diffusive activity from the lower mobility, particle-attached decay products. The theory of tube penetration will be presented along with a review of these initial studies.

Subsequently, the use of wire screens for the separation of the "unattached" fraction was developed by James *et al.* (1972), Thomas and Hinchliffe (1972) and George (1972). These systems were much easier to use although initially they suffered from the lack of a well developed theory to relate the screen properties to their collection efficiency. The collection efficiency of wire screens for the "unattached"  $^{218}\text{Po}$  was therefore empirically determined from calibration experiments using fresh  $^{218}\text{Po}$  in the absence of ambient aerosols, as a function of screen parameters and face velocity. George (1972) developed a standard method for measuring "unattached"  $^{218}\text{Po}$  fractions: a 60-mesh stainless steel screen is sampled simultaneously with a parallel filter, followed by  $\alpha$ -counting of both the screen and filter;  $^{218}\text{Po}$  data is extracted from both by the modified Tsivoglou technique and the "unattached" fraction is calculated as the ratio of twice the activity on one face of the screen to the activity on the filter. This method has been widely employed to obtain estimates of the "unattached" fraction in a variety of different environments.

The wire screen penetration theory developed by Cheng and Yeh (1980), Cheng *et al.* (1980) and Yeh *et al.* (1982) will be presented along with a semi-empirically corrected diffusion coefficient equation in the molecular cluster size range to characterize "unattached" fraction measurements reported by earlier studies. From these theoretical considerations, collection efficiency curves can be estimated for these measurements to demonstrate the potential for underestimation of the "unattached" cluster mode by the use of these methods and improvements in wire screen methods for such measurements are discussed in this context. The nature of respiratory deposition will then be presented along with the design concepts for a new sampling system that would yield measurements that can be directly related to dose with much greater accuracy.

## RELATIONSHIP BETWEEN PARTICLE SIZE AND DIFFUSION COEFFICIENT

The particle diffusion coefficient for aerosols is commonly estimated by the Einstein equation,

$$D = \frac{k T C}{3\pi\mu d_p} \quad (1)$$

where  $k$  is the Boltzmann constant ( $1.38 \times 10^{-16}$  erg  $^{\circ}\text{K}^{-1}$ ),  $T$  is the temperature in  $^{\circ}\text{K}$  (293 K at  $20^{\circ}\text{C}$  and 1 atmosphere),  $\mu$  is the gas viscosity ( $1.83 \times 10^{-4}$  gm  $\text{cm s}^{-1}$  for air) and  $C$  is the Cunningham correction factor given by Friedlander (1977),

$$C = 1 + \frac{\lambda}{d_p} [ 2.514 + 0.8 \exp(-0.55 d_p/\lambda) ] \quad (2)$$

where  $\lambda$  is the mean free path of the gas ( $0.65 \times 10^{-5}$  cm for air at 20°C).

Equation 2 was empirically derived to fit the entire range of values of  $d_p/\lambda$  from the continuum to the free molecular regimes (Davies, 1945). However, equations 1 and 2 overestimate the particle diffusion coefficient in the 0.5-1.75 nm particle diameter range. To illustrate this overestimation consider the diffusion coefficient for a  $^{222}\text{Rn}$  atom whose atomic diameter is estimated to be 0.46 nm. This diffusion coefficient was measured by Hirst and Harrison (1939) to be  $0.12 \text{ cm}^2 \text{ s}^{-1}$ . Equations 1 and 2 predict a diffusion coefficient of  $0.20 \text{ cm}^2 \text{ s}^{-1}$  for a 0.5 nm diameter cluster. This result is further evident from a comparison (Figure 1) with the diffusion coefficient as calculated using the kinetic theory of gases (Loeb, 1961, Porstendorfer, 1968, Raabe, 1969). The kinetic theory equation for the diffusion coefficient of molecular clusters in a gas,

$$D = \frac{0.815 V_r}{3 \pi s^2 N} [(M+m)/M]^{1/2} \quad (3)$$

where  $V_r$  is the root mean square velocity of the gas ( $5.02 \times 10^4 \text{ cm s}^{-1}$  for air at 20°C),  $N$  is the number concentration of gas molecules ( $2.51 \times 10^{19} \text{ cm}^{-3}$  for air at 760 mm Hg and 20°C),  $s$  is the sum of the radii of the gas molecules ( $0.155 \times 10^{-7} \text{ cm}$  for air) and of the cluster,  $M$  is the molecular weight of the cluster and  $m$  is that of the gas (28.9 for air).

In order to use a single equation for the particle diffusion coefficient over the entire size range, for  $d_p > 0.5$  nm, the Einstein-Cunningham equations 1 and 2 may be fitted to the kinetic theory equation 3 in the 0.5-1.75 nm size range in a manner that yields the original Einstein-Cunningham equations 1 and 2 for  $d_p > 1.75$  nm. This result may be obtained by the substitution of

$$d_p^* = d_p (1 + 3e^{-2.74 \times 10^7 d_p}) \quad (d_p \text{ in cm}) \quad (4)$$

for  $d_p$  in equation 2 for the Cunningham constant,  $C$ . The molecular weight-cluster size relationship for  $^{218}\text{Po}-\text{H}_2\text{O}$  clusters was used for the molecular weight factor,  $[(M+m)/M]^{1/2}$ , in the kinetic theory equation 3 to obtain the fitting parameter,  $d^*$ , in equation 4. Figure 1 is a plot of the corrected, uncorrected Einstein-Cunningham and kinetic theory diffusion coefficient

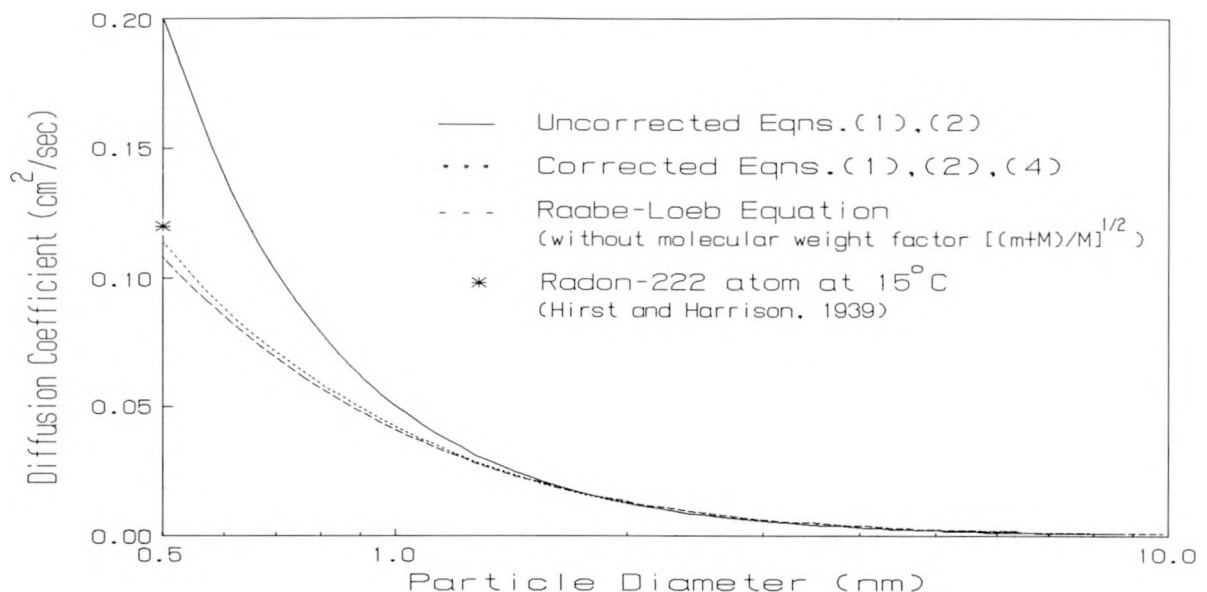


Figure 1. Diffusion coefficient for particles 0.5-10 nm in diameter, plotted using the uncorrected and corrected Einstein - Cunningham equations, and the kinetic theory equation without the mass factor,  $[(M+m)/M]^{1/2}$ .

equations versus particle diameter (the kinetic theory equation is plotted without the  $[(M+m)/M]^{1/2}$  factor which rapidly approaches unity).

## PENETRATION OF AEROSOLS THROUGH A TUBE

Theoretical equations for diffusional deposition in circular tubes are well-documented in the literature (e.g. Gormley and Kennedy, 1949; Fuchs, 1964). Of particular interest when sampling highly diffusive ultrafine cluster aerosols are tube penetration equations for the prediction of diffusional deposition or wall losses in the entrances of sampling tubes. Typically, the "wall loss" lengths,  $L$ , in these situations are smaller than the tube length required for the development of a laminar flow profile ("entrance length"). This entrance length,  $z$ , beyond which a parabolic flow field is established is (Fuchs, 1964),

$$z = 0.1 R \text{Re}_t \quad (5)$$

where  $R$  is the radius of the tube and  $\text{Re}_t = 2U_\rho R/\mu$  is the Reynolds number of the tube. Within this entrance distance,  $z$ , a developing flow exists and could enhance diffusional deposition. Theoretical studies by Tan (1969) and Chen and Comparin (1976) suggest that for

highly diffusive ultrafine cluster aerosols with small Schmidt numbers ( $S_c = v/D$ ) and penetration parameter,  $\mu^* = DL/R^2U < 0.05$  (small entrance length, L, and high flow velocity, U), assuming a uniform flow profile may be a suitable first-order approximation for the prediction of diffusional deposition losses.

Ingham (1975) developed an analytical, matched-asymptote solution for uniform flow penetration through a circular tube,  $P_t$ , given by,

$$P_t = \frac{4}{\alpha_1^2} e^{-\alpha_1^2 \mu^*} + \frac{4}{\alpha_2^2} e^{-\alpha_2^2 \mu^*} + \frac{4}{\alpha_3^2} e^{-\alpha_3^2 \mu^*} + \quad (6)$$

$$\{ 1 - 4 ( 1/\alpha_1^2 + 1/\alpha_2^2 + 1/\alpha_3^2 ) \} e^{-4 \mu^{*1/2} / [\pi^{1/2} (1 - 4 ( 1/\alpha_1^2 + 1/\alpha_2^2 + 1/\alpha_3^2 ))]}$$

The parameters  $\alpha_1^2$  ( $=5.783186$ ),  $\alpha_2^2$  ( $=30.471262$ ),  $\alpha_3^2$  ( $=74.887007$ ) are the zeros of the zero-order Bessel function of the first kind,  $J_0(\alpha_n) = 0$  (Tan, 1969). Equation 6 is valid for tube Reynolds number  $Re_t < 1200$  and tube Peclet number ( $Pe_t = RU/D$ )  $> 100$ .

Thomas (1955) attempted to verify the laminar flow tube penetration theory equations using gas molecules and reported agreement to within 20-30%. The discrepancies were attributed to experimental difficulties and possible entrance effects. Scheibel and Porstendorfer (1984) attempted a verification of tube penetration theory using monodisperse particles ( $d_p > 4$  nm). They reported good agreement with laminar flow theory (Gormley and Kennedy, 1949) for particle sizes greater than 15 nm and large deviations for particle sizes below 5 nm. The discrepancies were resolved by including terms for uniform flow deposition in the entrance of the tube, and for deposition on the front face of the tubes. Recent studies by Ramamurthi *et al.* (1990a) have found that tube penetration theory does accurately predict the deposition behavior of highly diffusive radioactive particles if the value of  $\mu^* \leq 0.05$ . For  $\mu^* > 0.05$ , equation 6 systematically underpredicts the penetration of particles through the tube. Figure 2 shows the results of this test of penetration of a single tube as a function of the diffusion parameter,  $\mu^*/D$ .

## DEPOSITION OF ULTRAFINE PARTICLES ONTO WIRE SCREENS

An equation of penetration through wire screens based on the theory of fibrous filtration was derived by Cheng and Yeh (1980) and Cheng *et al.* (1980). The penetration equation for a

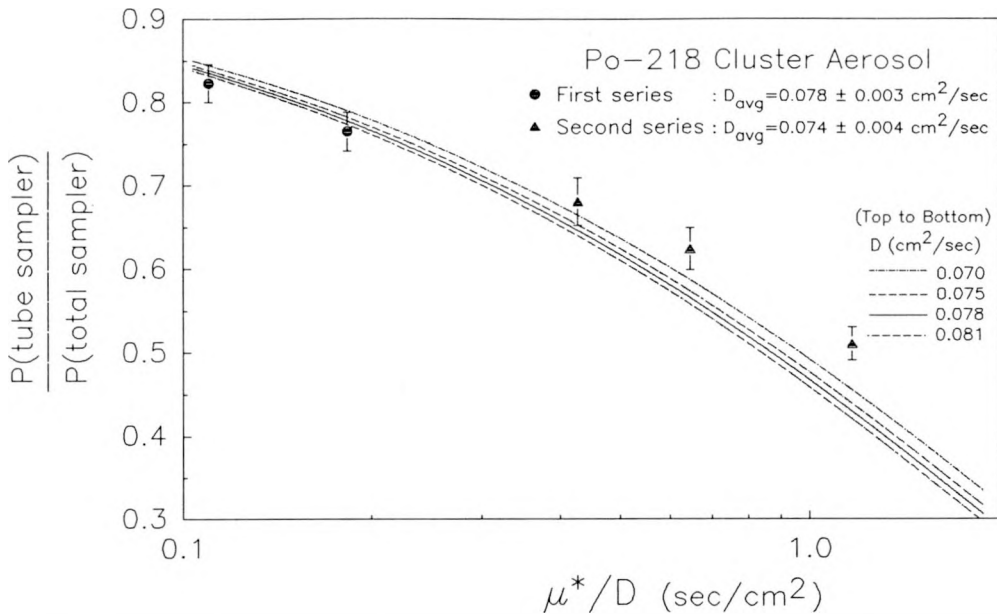


Figure 2. Assessment of penetration of radioactive particles into a cylindrical tube compared to the theoretical predictions of Ingham (1975).

wire screen, with wire diameter  $d_t$ , thickness  $w$ , volume fraction  $\alpha$  and sampling face velocity  $U$ , for ultrafine particles,  $d_p < 0.1 \mu\text{m}$ , is given by,

$$P = 1 - \eta = \exp \left[ - \frac{(4)(2.7)}{\pi} (KVF)^{-2/3} (D)^{2/3} \right] \quad (7)$$

where  $KVF = \frac{U}{[WF]^{1.5}}$  is the wire-velocity parameter ( $\text{cm}^2 \text{ s}^{-1}$ ),  $(8)$

$$WF = \frac{\alpha w}{(1-\alpha) d_t^{5/3}} \text{ is the wire factor } (\text{cm}^{-2/3}), \quad (9)$$

and  $D$  is the particle diffusion coefficient. Equation 7 is valid for wire Reynolds numbers ( $Re_t = U\rho d_t/\mu$ , where  $\rho$  is the density of air) less than 1 (Emi *et al.*, 1982). The fan model filtration theory has been applied to wire screens and experimentally verified for particle sizes  $d_p > 15 \text{ nm}$  ( $0.015 \mu\text{m}$ ) (Cheng and Yeh, 1980). Scheibel and Porstendorfer (1984) have further verified the fan model for particle sizes  $d_p \approx 4 \text{ nm}$ . Recent work with charged and uncharged  $^{218}\text{Po}$  clusters in the 0.5-1.5 nm size range has also indicated general agreement with the wire screen fan model penetration equation 7 (Holub and Knutson, 1987; Ramamurthi *et al.*, 1990a), although calibration studies remain necessary for  $d_p < 4 \text{ nm}$ . The penetration characteristics for

a wire screen operating in the 0.5-100 nm size range can thus be determined from equations 7, 8, and 9. Typical penetration curves are shown in Figure 3.

Further, each screen-velocity combination can be conveniently parameterized by its  $d_p(50\%)$  (Ramamurthi and Hopke, 1989), particle diameter for 50% collection efficiency, because of the form of the penetration in equation 7. This parameter can be determined (using a log-linear diffusion coefficient approximation) as,

$$d_p(50\%) \text{ (nm)} = 10^7 \exp \left[ - \frac{32.193 + \ln(KVF)}{1.957} \right] \quad (10)$$

for  $0.001 < KVF < 0.325$ .

## REVIEW OF PAST "UNATTACHED" FRACTION MEASUREMENTS

### Diffusion Sampler Measurements

#### INTRODUCTION

Most of the early work on "unattached" fraction measurements has been carried out in uranium mines. In the earliest studies including the work of Chamberlain and Dyson (1956), the "unattached" fraction was determined by measurement of the penetration of the activity through a right circular cylinder. Using the tube penetration theory of Gormley and Kennedy (1949), the fractional penetration can be related to a parameter given by  $\pi DL/2Q$ , where L is the length of the tube and Q is the volumetric flow rate through the tube. The diffusion coefficient of the radon decay products are assumed to have a single, very much larger value than the diffusion coefficients of the condensation nuclei to which the radon progeny becomes attached. Thus, by comparing the amount of activity penetrating through a tube of given dimensions at a given flow rate to the total airborne decay product activity, the fraction of "unattached" activities could be estimated.

The amount of "unattached" radioactivity has been measured in this manner by a number of investigators (Craft *et al.*, 1966; Fusamura *et al.*, 1967; Duggan and Howell, 1969). A problem that tends to confuse the literature of "unattached" fraction measurements is the number of ways in which the "unattached" radioactivity is reported. The ICRP has defined the "unattached" fraction as the fraction of the equilibrium number of  $^{218}\text{Po}$  ions which are unattached to particles (ICRP, 1959). However, the method used to measure the "attached" fraction readily yields the fraction of "unattached"  $^{218}\text{Po}$  atoms to the total number of  $^{218}\text{Po}$  atoms

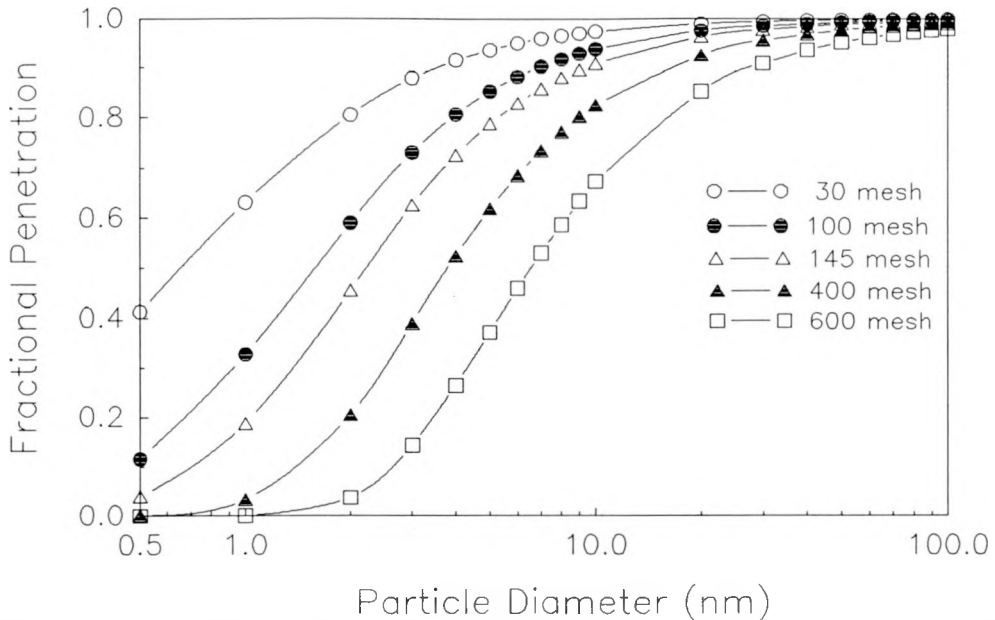


Figure 3. Fractional penetration through various mesh screens at a face velocity of  $10 \text{ cm s}^{-1}$ .

actually present. Chamberlain and Dyson (1956) made the first report of "unattached" fraction to be 0.1 using what became the ICRP definition (ICRP, 1959). It is important to carefully determine in each case what the investigator means by "unattached" fraction in order to compare results.

#### MINE ATMOSPHERES

Craft *et al.* (1966), using a diffusion sampler and an assumed diffusion coefficient of  $0.045 \text{ cm}^2 \text{s}^{-1}$ , found a wide range of fractions of 0 to 0.73. However, they defined their fraction as the fraction of "unattached" radon daughter alpha energy concentration to the total radon decay products alpha energy concentration. They conclude that there is so much variability from location to location and mine to mine that it is not possible to select any particular value of "unattached" activity as being representative of actual mine conditions. They do observe that in the presence of diesel smoke, the "unattached" fractions were low.

Fusamura *et al.* (1967) also used a tube diffusion sampler. They assumed a diffusion coefficient of  $0.054 \text{ cm}^2 \text{s}^{-1}$  and found fractions of  $^{218}\text{Po}$  from 0.06 to 0.13 in active mine areas where dust producing activities were in progress and from 0.09 to 0.25 in inactive areas of mines according the ICRP definition. They found that drilling operations produced substantial oil

mists to which the radon progeny attached. In areas with pneumatic loaders or picks, the "unattached" fractions were in the 0.09 to 0.13 range. It was anecdotally reported that in areas where no work was being done, the "unattached" fraction reached as high as 0.5, but no specific number was reported related to their measurements in particular locations in several mines.

George and Hinchliffe (1972), George *et al.* (1975), and George *et al.* (1977) of the Health and Safety Laboratory (HASL, now the Environmental Measurements Laboratory) describe an extensive series of measurements in active uranium mines in the Grants mineral belt of New Mexico. In these studies, they used a diffusion sampler that is based on the studies of deposition of "unattached" radon progeny in an impactor stage (Mercer and Stowe, 1969). The collection efficiency as a function of sample flow rate is given in Figure 4. However, Subba Ramu (1980) has built a similar device and he suggests that the device is about 90% efficient at  $1 \text{ L min}^{-1}$ . He claims that the difference in efficiencies between the HASL devices described by George and Hinchliffe (1972) and his sampler were due to his "extreme precautions to minimize the presence of attached radon daughter products, which interfere with accurate calibration." Thus, there exists some uncertainty in these measurements and may underpredict the "unattached" fractions.

The results of the series of measurements are summarized in Figures 5 and 6. Figure 5 shows the "unattached" fractions of  $^{218}\text{Po}$ ,  $f_a$ , as defined by the ratio of the total  $^{218}\text{Po}$  activity collected in the sampler divided by the collection efficiency times the total airborne  $^{218}\text{Po}$  activity as measured on an open face filter. Figure 6 shows the "unattached" fraction as defined by ICRP (1959). These values are obtained by multiplying the  $f_a$  values by the ratio of the total airborne  $^{218}\text{Po}$  activity concentration (pCi/L) to the radon concentration (pCi/L). It should be noted that the ICRP "unattached" fraction values are substantially lower than the fraction of  $^{218}\text{Po}$  that is "unattached".

Cooper *et al.* (1973) also used a Mercer and Stowe diffusion sampler to measure "unattached" fractions in mines. They examined a mine in the Uravan Belt area of Colorado (Mine A) and a mine in the Ambrosia Lake, New Mexico (Grants mineral belt) (Mine B). The results of these studies also included detailed inorganic and organic analyses of the collected particulate matter. Only 13 "unattached" fraction measurements are reported; 10 in mine A and 3 in mine B. Their results are summarized in Figure 7.

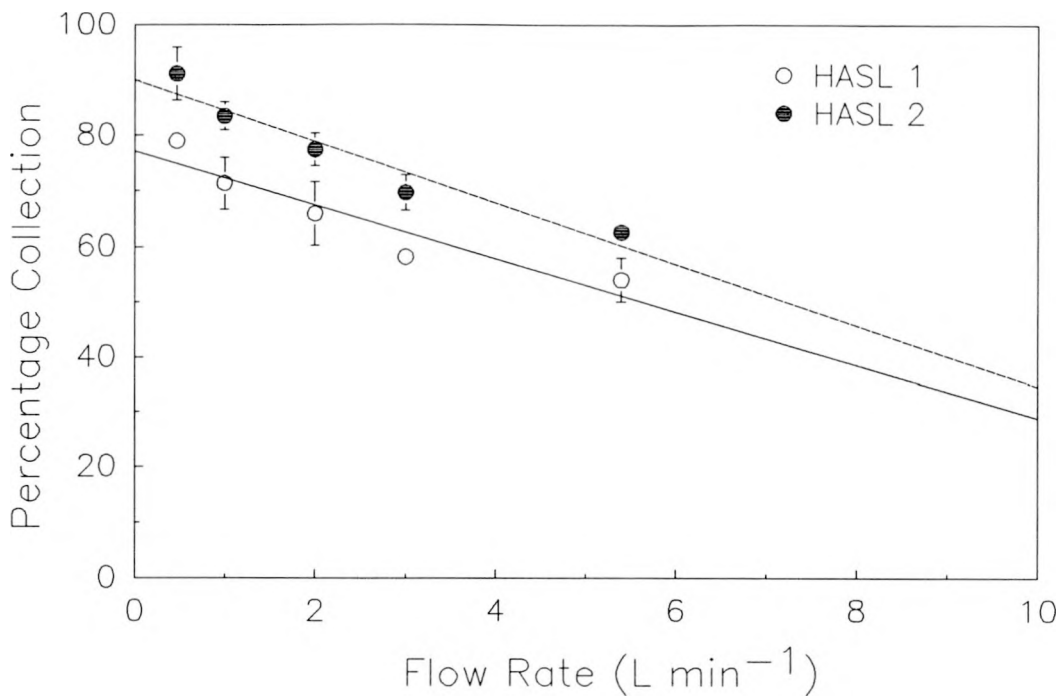


Figure 4. Collection efficiency of the HASL diffusion samplers for  $^{218}\text{Po}$  as a function of flow rate redrawn from data in George and Hinchliffe (1972). The lines are simple first order regression lines drawn through each set of points.

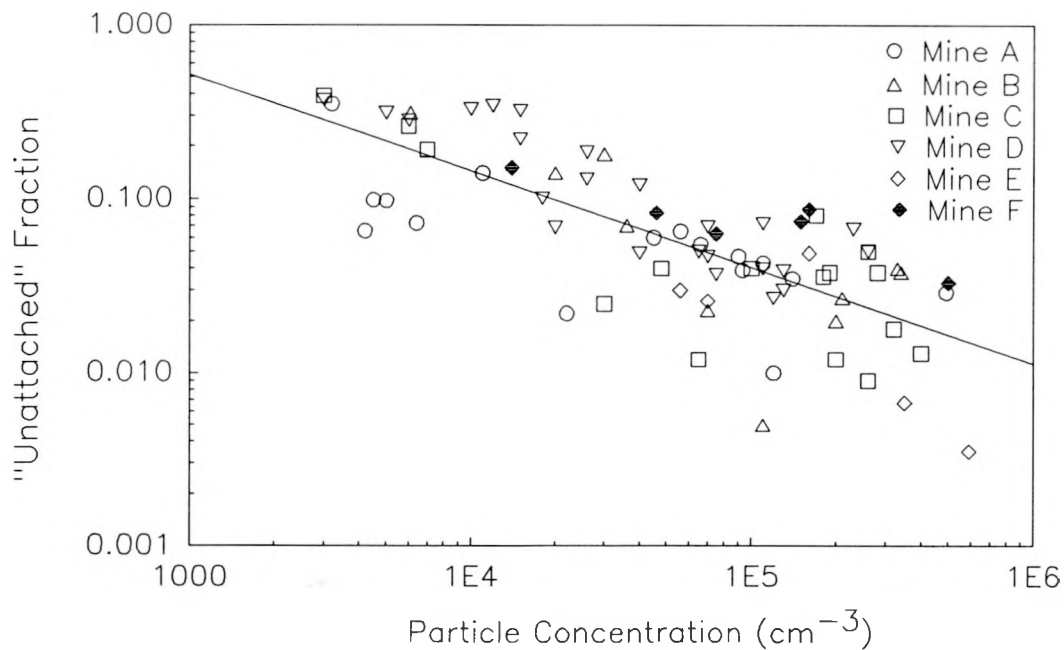


Figure 5. "Unattached" fraction of  $^{218}\text{Po}$  as defined by ICRP (1959) measured in New Mexico uranium mines as a function of particle concentration. Data for this plot was taken from George and Hinchliffe (1972) and George *et al.* (1977).

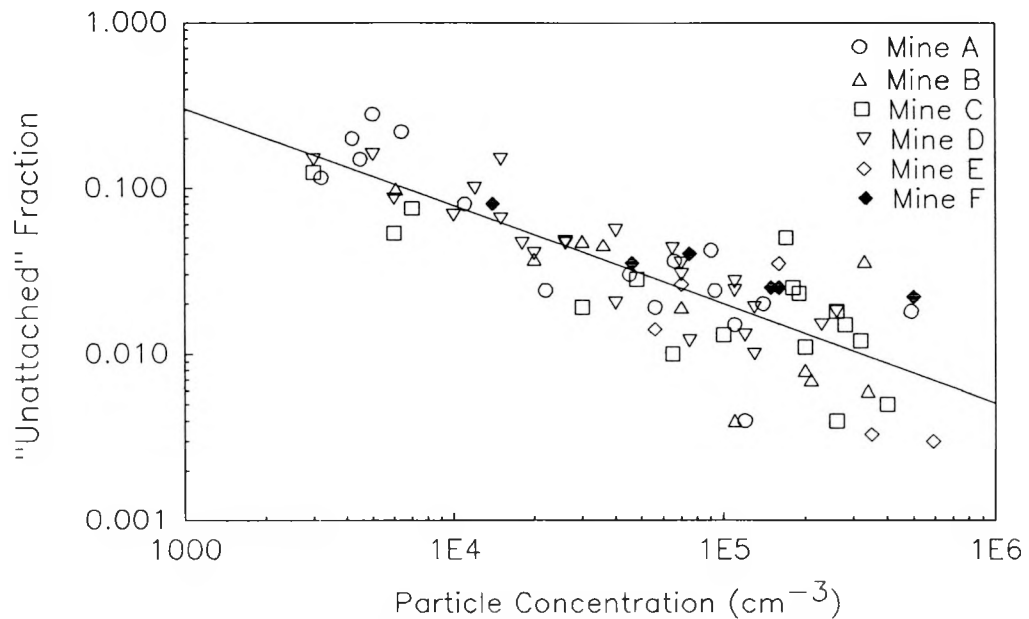


Figure 6. "Unattached" fraction of  $^{218}\text{Po}$  as defined relative to total  $^{218}\text{Po}$  measured in New Mexico uranium mines as a function of particle concentration. Data for this plot was taken from George and Hinchliffe (1972) and George *et al.* (1977).

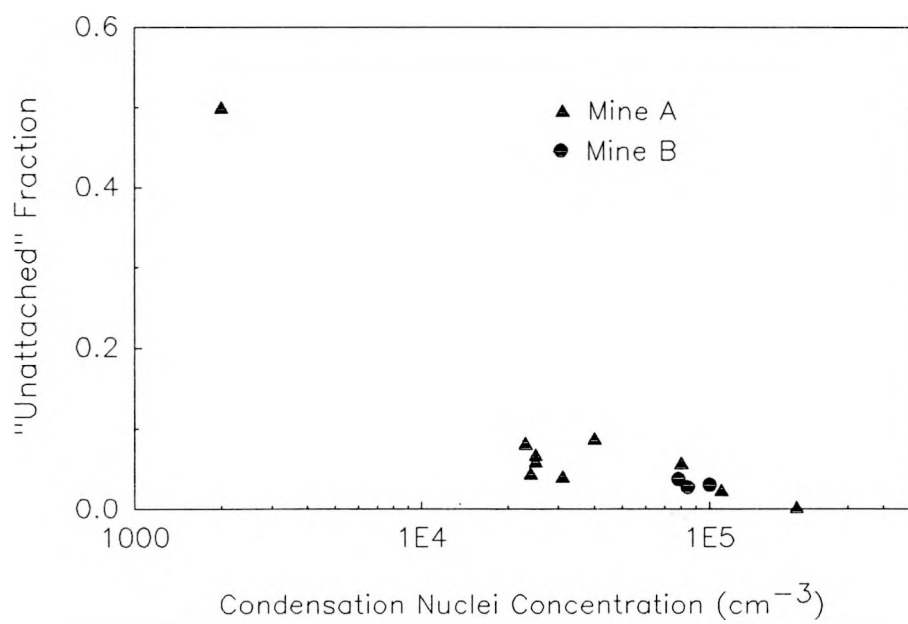


Figure 7. "Unattached" fraction measurements of Cooper *et al.* (1973). All of the results are the fraction of  $^{218}\text{Po}$  activity that is "unattached."

## AMBIENT AND INDOOR ATMOSPHERES

Duggan and Howell (1969) first attempted to use electrostatic collection of the decay products to determine the "unattached" fractions. However, as is now known (Hopke, 1989a & b), neutralization of the decay products is sufficiently rapid in normal air that only a small fraction of the highly diffusive fraction of the activity is charged. They then used a rectangular channel diffusion battery to remove the "unattached" activity. The battery had 28 channels of cross-section 0.07 cm by 5 cm and operated at a flow rate of  $80 \text{ L min}^{-1}$ . The penetration curve for their battery is shown in Figure 8. They measured the "unattached" fraction in outdoor and laboratory air at quite low radon concentrations (0.04 to 0.39 pCi/L). In the approximately 50 measurements that were made, they obtained values in the range of 0.07 to 0.40 with no discernable relationship between "unattached" fraction and the radon concentration. No measurements of the condensation nuclei concentrations are reported nor was there any apparent attempt made to obtain size distribution results from the measurements. Thus, it is difficult to use these values to assess the exposure to "unattached" progeny in either the ambient atmosphere or in indoor air.

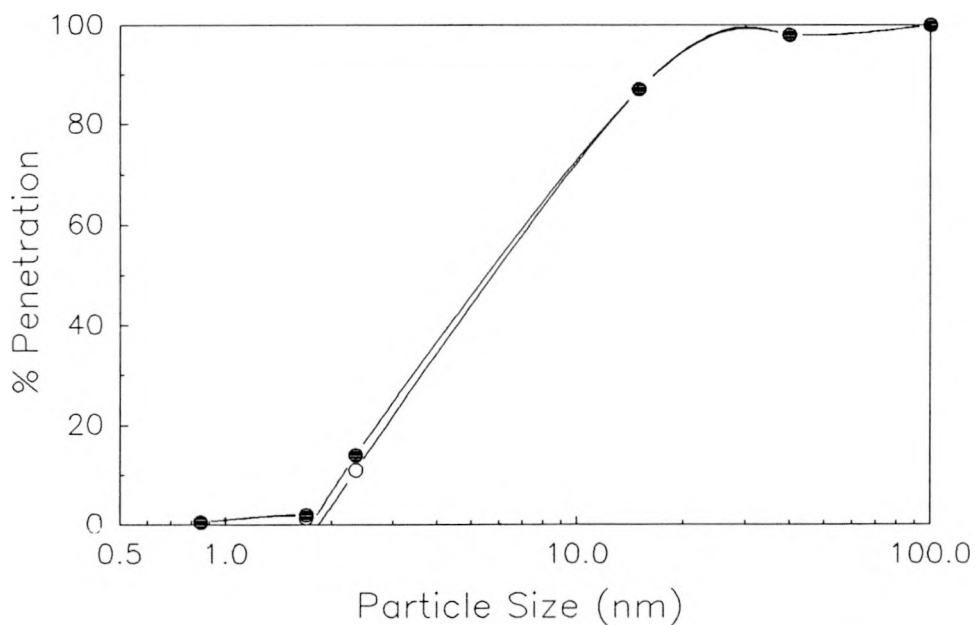


Figure 8. Calculated penetration values for the Duggan and Howell (1969) diffusion battery. Open circles represent the initial calculation. Filled points are for a recalculation made to include the measured non-uniformity of inlet airflow.

Shimo and Ikebe (1984) and Shimo *et al.* (1985) present results of "unattached" fraction measurements in an underground tunnel of the Mikawa Crustal Movement Observatory of Nagoya University using a diffusion tube. They then used the tube as the body of a proportional counter and followed the decay of the alpha activity in order to extract the concentrations of the three decay products. The total activity of each decay product was determined using the Thomas-modified Tsivoglou method (Thomas, 1970). Radon concentrations were in the range of 73.5 to 251 pCi/L. The aerosol concentrations were measured with a Pollak-type condensation nuclei counter and were found to be in the range of 2,000 to 10,000 cm<sup>-3</sup>. The "unattached" fraction of <sup>218</sup>Po compared to total <sup>218</sup>Po was determined as  $0.49 \pm 0.14$ ; of <sup>214</sup>Pb was  $0.067 \pm 0.019$ ; and of <sup>214</sup>Bi was  $0.032 \pm 0.009$ . The "unattached" fraction of potential alpha energy concentration was 0.12 with a range of 0.09 to 0.14.

### Wire Screen Measurements

#### INTRODUCTION

The diffusion samplers were fairly cumbersome devices to use and therefore a simpler and more portable system was developed based on the collection of the activity on wire mesh screens. Wire mesh screens have become the most commonly used method for estimating "unattached" Rn daughter fractions. The early development of these systems was described by James *et al.* (1972), Thomas and Hinchliffe (1972), and George (1972). Thomas and Hinchliffe (1972) also developed a semi-empirical equation for the "unattached" <sup>218</sup>Po collection efficiency of wire screens that was widely used by researchers before the development of equation 7. The Thomas-Hinchliffe equation, compared to the Cheng-Yeh equation 7, overestimates wire screen collection efficiencies for particle diameters,  $d_p < 1.0\text{-}2.0$  nm and  $d_p > 5.0\text{-}7.0$  nm, for most screen-velocity combinations. A comparison of the Thomas-Hinchliffe equation compared to the Yeh-Cheng theory is provided in Figure 9.

A number of wire screen measurement studies of the "unattached" <sup>218</sup>Po fraction are reported in the literature (James *et al.* 1972, George 1972, Raghavayya and Jones 1974, Bigu and Kirk 1980, Strandén and Berteig 1982, Bigu 1985, Reineking *et al.* 1985). Table 1 is a compilation of the wire screen parameters and face velocities used in these studies. Each screen-velocity combination is characterized by its  $d_p(50\%)$  parameter obtained from equation 10. Nominal values for commonly undocumented parameters such as  $w$  and  $\alpha$  were taken from

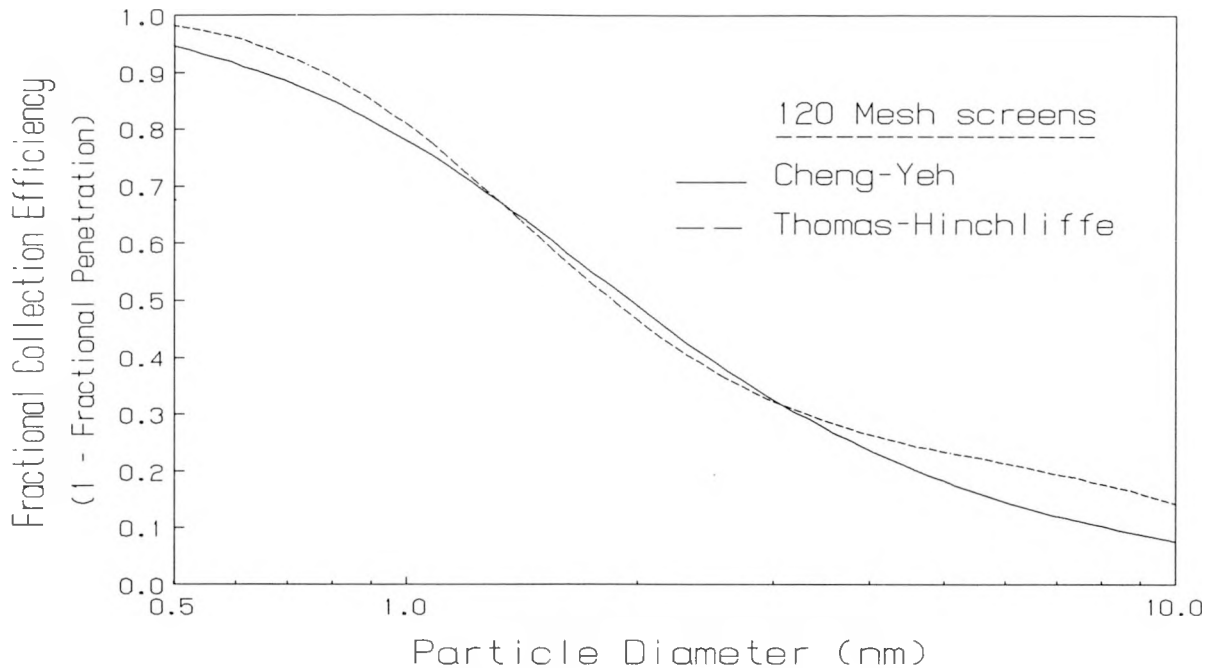


Figure 9. Comparison of Thomas-Hinchliffe empirical calibration and Yeh-Cheng screen penetration for a 120 mesh at a face velocity of  $10 \text{ cm-s}^{-1}$ .

wire screen manufacturers' catalogs for screens with the appropriate combination of mesh number and wire diameter reported in the studies.

Figure 10 shows the calculated particle collection efficiency characteristics for each of the studies listed in Table 1, determined using the Cheng-Yeh theory discussed earlier. The collection efficiencies for the 60 mesh screens used by George (1972) and the 150 mesh screens used by Bigu (1985) are also plotted, although the wire Reynolds numbers are greater than 1. Wire screens with collection efficiencies that differ only slightly have been plotted together for comparison purposes. The collection efficiencies of the screens are between 70-90% and 6-12%, respectively, for 1 nm and 10 nm diameter particles and decrease rapidly in the 1-3 nm size range.

The concept of an "unattached" fraction measurement is to have a system that will collect all of the highly diffusive activity without collecting any activity attached to "particles." The separation of aerosol size distributions into well defined modes has been used to great advantage in studying the much larger sized modes ( $\geq 1 \mu\text{m}$ ) in the ambient aerosol. However, such measurements are possible because the separation of large particles are based on their

Table 1. Wire screen parameters and face velocities used in published wire screen "unattached" fraction measurements. Underestimation of "unattached" fraction is based on a log-normally distributed mode with  $d_m=1.0$  nm and  $\sigma_g=1.5$ .

Study	MESH $d_f$ NO.	U ( $\mu\text{m}$ )	$d_p(50\%)$ (nm)	"Unattached" Mode	
				Underestimation [ $\frac{100 - \% \text{ Coll.}}{\% \text{ Coll.}}$ ]	(%)
James et al. (Ja72) (1972)	200	50.8	12.0	2.7	15
George (1972) (Ge72a)	60	178.0	11.5	1.7	45
George (1972) (Ge72b)	80	127.0	11.5	1.9	36
Raghavayya and (Ra72) Jones (1974)	120	94.0	12.2	2.0	29
Bigu and Kirk (Bi80) (1980)	150	76.0	9.6	2.8	14
Stranden and (St82) Berteig (1982)	174	56.0	21.0	2.3	22
Bigu (1985) (Bi85)	150	76.0	27.3	1.6	48
Reineking <i>et al.</i> (Re85) (1985)	188	50.0	8.5	2.0	31

Nominal values for  $w$  and  $\alpha$  obtained from screen manufacturers' catalogs.

inertial properties. In this case devices with sharp cut-points such as cyclones or impactors can be designed (Lodge and Chan, 1986). However, because of the stochastic nature of diffusional deposition, the collection curves for wire screens or tubes are much more gradual functions of particle size. To illustrate the problem with using a single screen for making such a dichotomous measurement, Figure 11 shows the collection efficiency curves with  $d_p(50\%)$  along with the characteristics of a log-normally distributed aerosol with a median diameter of 1.0 nm and a geometric standard deviation of 1.5 in the range suggested by Reineking and

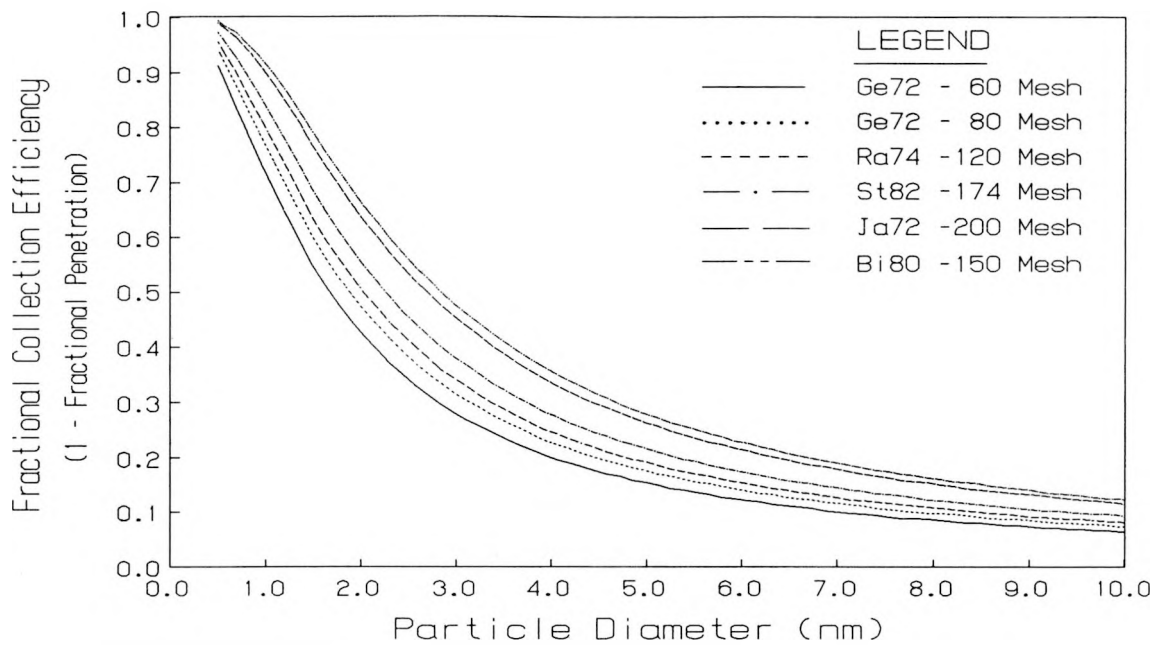


Figure 10. Collection characteristics for the wire mesh screen systems used in a number of the reported "unattached" fraction measurements.

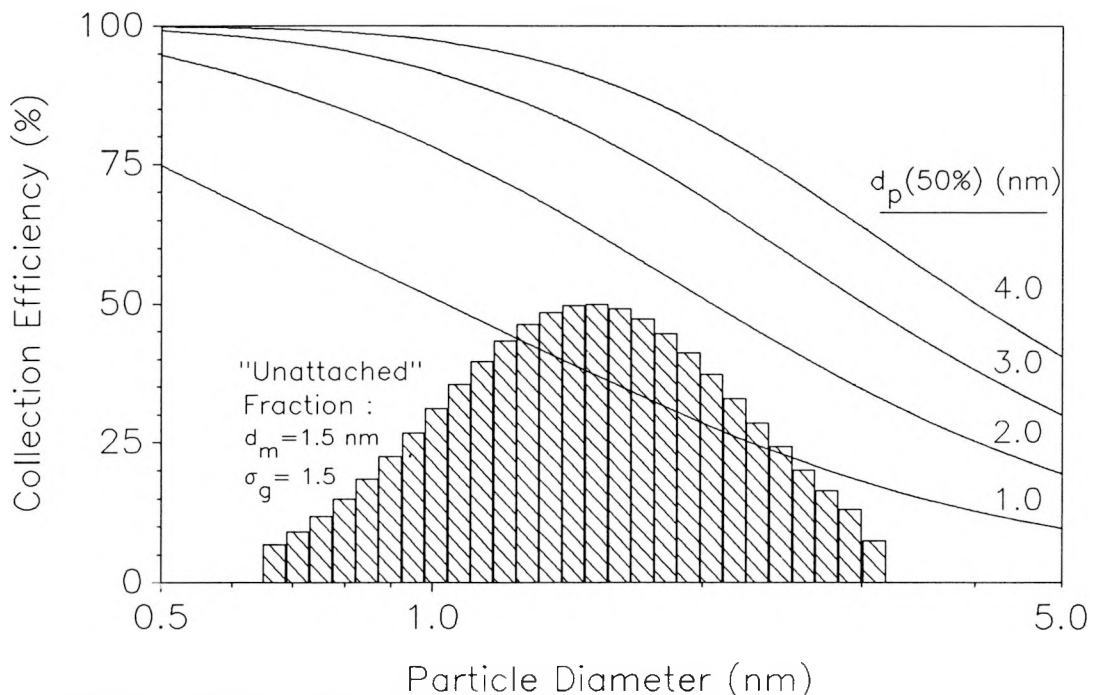


Figure 11. Collection efficiency curves for "typical" wire screens characterized by  $d_p(50\%)$  values of 1, 2, 3, and 4 nm and presentation of a log-normal size distribution characteristic of the "unattached" fraction.

Porstendorfer (1986).

It can be seen that the use of wire screens will underestimate the "unattached" fraction if it indeed consists of an ultrafine cluster mode in the 0.5-3 nm size range (Reineking and Porstendorfer 1986). The cumulative collection of activity as a function of size is presented in Figure 12. The underestimation of the "unattached" cluster mode in each of the studies is presented in Table 1. The wire screens used in these studies would underestimate such an "unattached" cluster mode by 14-48%, depending on the  $d_p(50\%)$  parameter for the particular screen-velocity combination. The choice of a single, optimized screen  $d_p(50\%)$  parameter that maximizes the collection of the "unattached" mode while minimizing the collection of "attached" activity may hence be beneficial for single screen "unattached" fraction measurements.

To facilitate the appropriate choice of this parameter, the collection efficiency of a log-normally distributed aerosol particle mode was determined as a function of wire screen  $d_p(50\%)$  as shown in Figure 12. It appears from this figure that a wire screen  $d_p(50\%) = 4$  nm is an optimal choice yielding about 90% collection of the "unattached" mode ( $d_m = 1$  nm,  $\sigma_g = 1.5$ ,  $0.5 < d_p < 3$  nm), while minimizing the collection of activity in the second aerosol mode ( $d_m = 25$  nm,

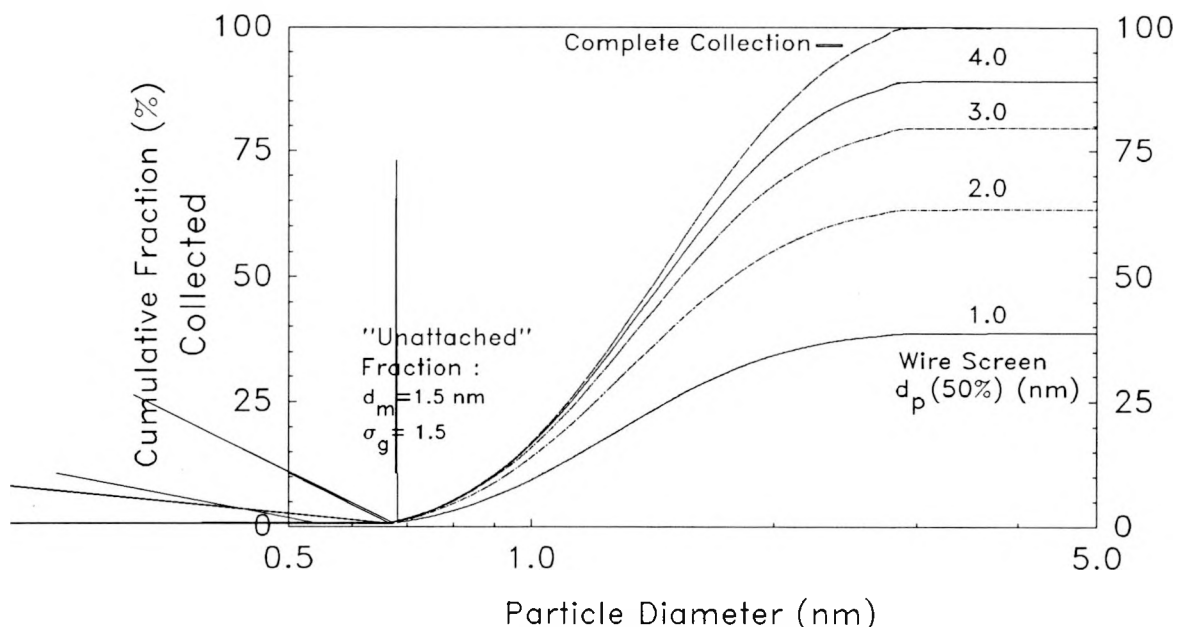


Figure 12. Cumulative collection fraction of an ultrafine activity mode having a median diameter of 1.0 nm and geometric standard deviation of 1.5 for various wire screen systems characterized by their  $d_p(50\%)$  values.

$\sigma_g=1.75$ ,  $10 < d_p < 60$  nm) to less than 8%. Activity in the latter size range may be significant in indoor air following cooking, as reported by Tu and Knutson (1988a). The collection of activity "attached" to the larger aerosol particle mode ( $d_m=125$  nm,  $\sigma_g=2.0$ ,  $40 < d_p < 400$  nm) is minimal for  $d_p(50\%) < 10$  nm, and is about 1% for  $d_p(50\%) = 4$  nm. This result is consistent with the calculations by Van der Vooren *et al.* (1982) for the collection of "attached" activity in this size range by wire screens sampling the "unattached" mode. In sampling dusty atmospheres with particle sizes,  $d_p > 0.5 \mu\text{m}$  (500 nm), collection by impaction and interception may become significant, but for wire screens with  $d_f > 100 \mu\text{m}$ ,  $\alpha < 0.3$  and  $U < 10.0 \text{ cm s}^{-1}$  the wire screen collection efficiency for a  $5 \mu\text{m}$  particle is less than 5%. More recent work by Reineking and Porstendorfer (1990) suggests that there can be errors in "unattached" fraction measurements caused by inertial collection of radioactivity-carrying particles  $> 100$  nm.

Another consideration of wire screen systems are the activity measurements. Measurement of the activity collected by a wire screen is complicated by the deposition of activity on the front and back faces of the screen as well as alpha absorption losses in the screen weaves. The ratio of activity collected on the front and back faces of a wire screen has been found to be clearly dependent on both the screen parameters and the activity distribution sampled by the screen (Holub and Knutson 1987). For single wire screen samplers, analysis of the total or reference filter ( $A_t$ ) and the wire screen backup filter ( $A_{bf}$ ) activities would yield more reliable estimates of the "unattached" fraction and would help circumvent the problems associated with analyzing the wire screens themselves for collected activity. However, depending on the amount of activity that attaches to the screen may lead to low statistical precision in the activity determination on the screen back-up filter.

## MINE ATMOSPHERES

Raghavayya and Jones (1974) made measurements in three mines in Colorado and New Mexico of radon, decay product concentrations, "unattached" fractions of each decay product, and condensation nuclei concentration. They used the Thomas and Hinchliffe (1972) approach to calculate collection efficiency. However, since they calculate that they will obtain 92.59% collection for  $D=0.06 \text{ cm}^2\text{s}^{-1}$  activity, they assume in the high particle concentration atmospheres in the mine, there is 100% collection of "unattached" and no collection of "attached" activity. They counted the wire screens and had difficulties getting the total activity measured with a

separate filter to match the sum of the activity on the screen plus that on the backup filter.

They developed an empirical correction factor of the form

$$\tan (0.9f_a) = k_1 W + k_2 \quad (11)$$

where  $k_1$  and  $k_2$  are constants depending on which decay product is being measured, and  $W$  is the ratio of the activity on backup filter to that on the screen. This approach was then used on the mine data to obtain the values they present. They present the data as the fraction of activity for each decay product that is "unattached" and a total "unattached" fraction relative to radon.

$$f_t = \frac{T_a F_a f_a + T_b F_b f_b + T_c F_c f_c}{T_a F_a + T_b F_b + T_c F_c} \quad (12)$$

Mercer (1975) has noted that the form of a correction factor in equation 12 leads to minimum values of  $f_a$ . He provides an alternative analysis of their calibration data and a new set of  $f$  values. These values are presented in Figure 13 as a function of the condensation nuclei count as measured with a Gardner CN counter. However, other problems have been noted in the results. Kotrapa and Mayya (1976) has examined the equations used to calculate the  $^{218}\text{Po}$ ,  $^{214}\text{Pb}$ , and  $^{214}\text{Bi}$  concentrations and found errors in the Raghavayya and Jones equations. They

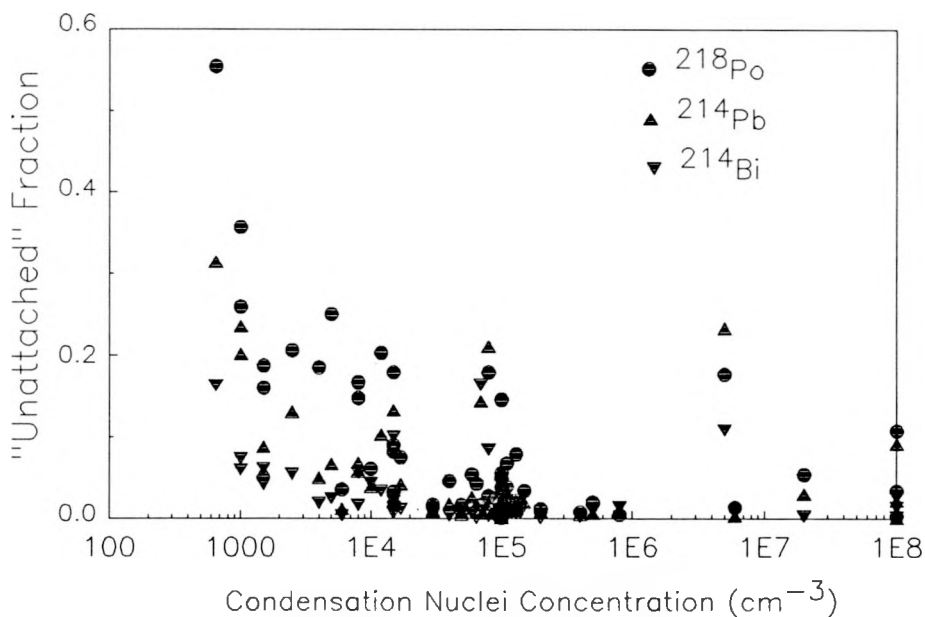


Figure 13. "Unattached" fraction measurements of Raghavayya and Jones (1974) as corrected by Mercer (1975) as a function of particle concentration.

have recalculated the concentrations of the decay products, working levels, and a revised set of total "unattached" fractions that they incorrectly describe as following the ICRP (1959) definition. The corrected total "unattached" fractions are presented as a function of the condensation nuclei concentration in Figure 14.

In general, the  $^{218}\text{Po}$  results show the largest "unattached" fraction compared to the longer-lived  $^{214}\text{Pb}$  and  $^{214}\text{Bi}$ . The ranges of the fractions of "unattached" atoms to atoms present are as follows:

$$0.0013 < f_{^{218}\text{Po}} < 0.554$$

$$0.0006 < f_{^{214}\text{Pb}} < 0.314$$

$$0.0008 < f_{^{214}\text{Bi}} < 0.164$$

Further examination of the Raghavayya and Jones (1974) results still suggest problems in their measurements. For example, it would be expected that as the condensation nuclei count increases, there should also be an increase in the equilibrium fraction as defined by

$$F = \frac{0.105c_a + 0.516c_b + 0.379c_c}{c_{Rn}} \quad (13)$$

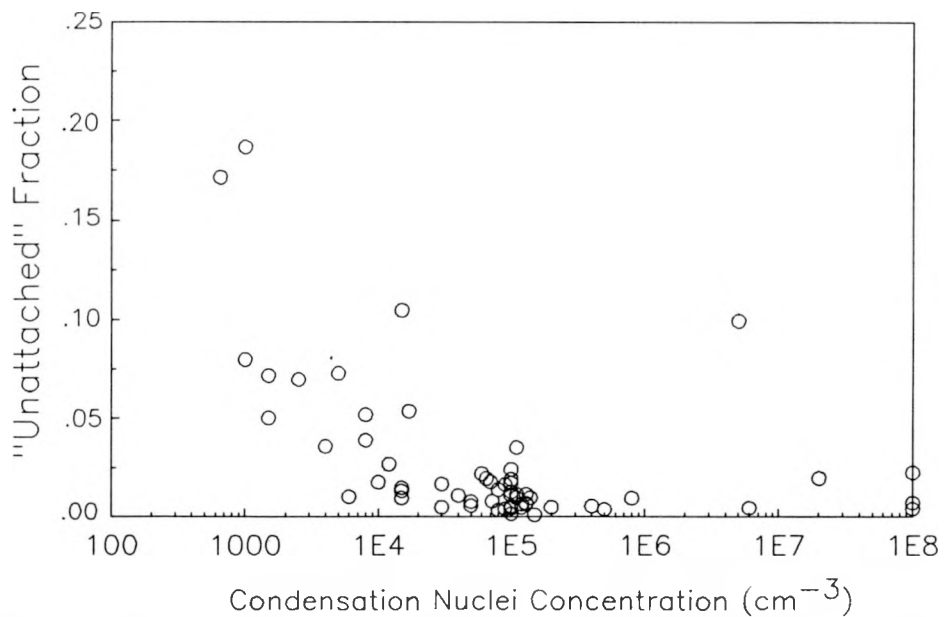


Figure 14. Total "unattached" fraction,  $f_u$ , as measured by Raghavayya and Jones (1974) with corrected values of Kotrappa and Mayya (1976).

The equilibrium fraction as a function of condensation nuclei concentration is presented in Figure 15. It can be seen that there is no clear trend in the data. From prior measurements of attachment coefficients (Raabe, 1969; Porstendorfer and Mercer, 1979), it would be anticipated that there should be a substantial increase in the equilibrium factor with increasing particle concentrations. These results thus suggest a substantial problem in either the radon progeny measurements or the field measurements of the number of condensation nuclei.

Bigu and Kirk (1980) have measured "unattached" fractions in two Canadian mines using both a diffusion sampler and a wire screen system. The collection efficiencies of the diffusion and wire screen samplers were reported to be 53% and 95%, respectively, when operated at a  $2 \text{ L min}^{-1}$ . Their  $^{218}\text{Po}$  "unattached" fraction results are presented in Table 2. In general, there is reasonable agreement between the two measurements. Unfortunately, there are only limited condensation nuclei measurements and no radon measurements were reported. Thus, the ICRP f values cannot be calculated nor can the equilibrium fraction be determined. The values are similar to the other values reported for active working areas of mines.

Other measurements were performed in one Canadian mine by Busigin *et al.* (1981b). They used a parallel plate diffusion batteries. Their measurements were in active mining areas

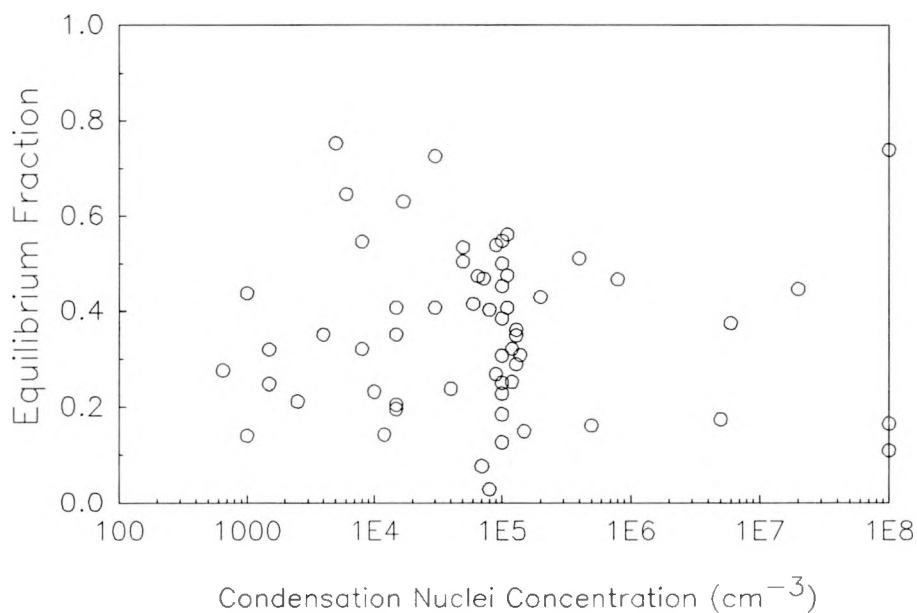


Figure 15. Equilibrium fraction calculated from the data of Raghavayya and Jones (1974) as corrected by Kotrappa and Mayya (1976) as a function of the condensation nuclei count.

Table 2. "Unattached" fraction measurements reported by Bigu and Kirk (1980).

Mine	Test No. <sup>a</sup>	D.S. <sup>b</sup>	W.S. <sup>c</sup>	"Unattached" Fraction Nuclei (cm <sup>-3</sup> )	Condensation Operation	Mining Mine	Area of
A	1		.09	.07	2.5x10 <sup>5</sup>	Drilling & Slushing	'Non-Diesel'
B	2		.064	-	3.0x10 <sup>5</sup>	Drilling	'Non-Diesel'
A	3		.058	-	-	Drilling	'Non-Diesel'
A	4		.014	.025	-	Roof Bolting	'Non-Diesel'
A	5		.0047	.0047	-	Mucking	'Diesel'
A	6		.006	.0025	-	Mucking & Drilling	'Diesel'
A	7		.0067	.007	-	Mucking, Drilling, & Roof Bolting	'Diesel'

<sup>a</sup> Each test represents one day during which a number of measurements were made.

<sup>b</sup> Diffusion sampler measurements.

<sup>c</sup> Wire screen measurements.

with high particle concentrations (approximately  $10^6$  nuclei  $\text{cm}^{-3}$ ). Under these conditions, they found no distinct "unattached" fractions with an upper limit of 1 to 2%. Subsequently, the same group has made more extensive measurements in two mines using a wire screen sampler (Khan *et al.*, 1987). Although this paper followed the publication of the detailed theory of wire screen collection in the early 1980s, this group continued to use the Thomas and Hinchliffe collection efficiency curve. Thus, the penetration efficiencies have some error and lead to an underestimation of the "unattached" fraction by approximately 10 to 15%. Subsequent measurements by Bigu (1985) also found very small values of "unattached" progeny ( $\leq 0.01$ ) with aerosol concentrations in excess of  $10^5 \text{ cm}^{-3}$ .

Stranden and Berteig (1982) made a series of 33 measurements in an iron ore mine in Norway. They also use the Thomas and Hinchliffe collection efficiency and report the fractions

of "unattached"  $^{218}\text{Po}$ ,  $^{214}\text{Pb}$ , and  $^{214}\text{Bi}$  and the fraction of "unattached" potential alpha energy concentration (PAEC). The "unattached" PAEC is obtained from the individual concentrations as follows:

$$f_p = \frac{1.05 C_a^f + 5.16 C_b^f + 3.8 C_c^f}{1.05 C_a + 5.16 C_b + 3.8 C_c} \quad (14)$$

The distribution of values for these four variables are presented in Figure 16. In this case, condensation nuclei concentrations were not measured. However, they did obtain very reasonable relationships for  $f_a$  and  $f_p$  with the respirable dust concentration (particles  $< 7 \mu\text{m}$ ) in  $\text{mg m}^{-3}$ . Their results are summarized in Table 3.

#### AMBIENT AND INDOOR ATMOSPHERES

Only a limited number of measurements of "unattached" fractions in single family homes, apartments, offices, and other non-mine locations have been performed. Porstendörfer and coworkers (Reineking *et al.*, 1985; Reineking and Porstendörfer, 1986; Porstendörfer, 1987; Reineking and Porstendörfer, 1990) have made measurements of both "unattached" fraction and the total activity size distribution for a series of rooms in unoccupied houses. In these studies, they have varied the ventilation rate and added aerosol sources to the room. From the results of the measurements on the radon progeny, radon, and particle concentrations, they have then calculated the "unattached" fraction of  $^{218}\text{Po}$ ,  $^{214}\text{Pb}$ , and potential alpha energy and the

Table 3. Values for the mean and median "unattached" fractions as measured in a Norwegian iron ore mine by Strandén and Berteig (1982).

Species	Mean	Median
$^{218}\text{Po}$	0.123	0.063
$^{214}\text{Pb}$	0.057	0.032
$^{214}\text{Bi}$	0.032	0.018
PAEC	0.059	0.038

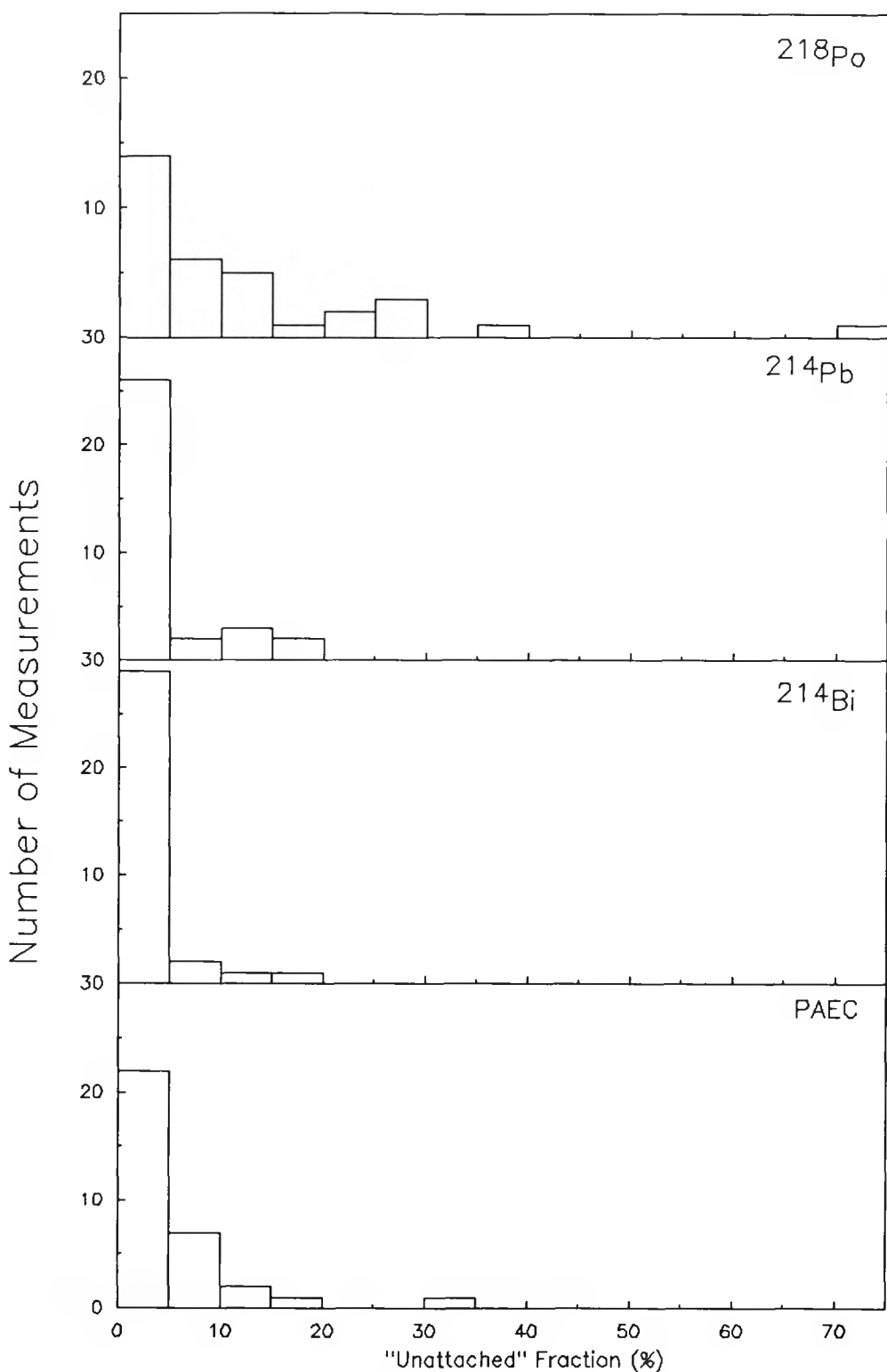


Figure 16. Distributions of the "unattached" fractions of the three radon decay products and PAEC measured in an iron ore mine. Redrawn from the graph in Strandén and Berteig (1982).

equilibrium fractions. The results of the "unattached" fraction of PAEC as a function of condensation nuclei concentration in five rooms with and without aerosol sources are shown in Figure 17. Figure 18 presents the equilibrium factor as a function of particle concentration for these same rooms. In their later reports (Porstendorfer, 1987), three additional rooms have been characterized with similar results. In their most recent report, Reineking and Porstendorfer (1990) also provide some results for a limited number of measurements in the ambient atmosphere. These results are presented in Table 4.

Vanmarcke *et al.* (1985; 1987; 1989) have utilized a screen diffusion battery with characteristic  $d_p(50\%)=4$  nm for "unattached" fraction measurements in indoor air. In addition aerosol size distributions are made with an automated aerosol spectrometer system (Raes *et al.* (1984). They measured the "unattached" fraction of PAEC and reported that their results indicate "that the fraction of unattached radon daughters is higher than assumed in earlier studies". A sequence of "unattached" fraction measurements made in a single Belgian house is shown in Figure 19 (Vanmarcke *et al.*, 1985). Additional studies made in the same house and in several other locations including their laboratory and a railroad station as well as a second room. Figure 20 summarizes the equilibrium and unattached fraction measurements plotted as a function of the attachment rate inferred from the aerosol number distribution. Unfortunately,

Table 4. Concentrations of radon, "attached" and "unattached" activities,  $f_p$ , F-values and particles measured in the ambient atmosphere near Göttingen (1 m above the ground during daylight) by Reineking and Porstendorfer (1990).

Period	$^{222}\text{Rn}^a$ ( $\text{Bqm}^{-3}$ )	$^{218}\text{Po}^a$ ( $\text{Bqm}^{-3}$ )	$^{218}\text{Po}^f$ ( $\text{Bqm}^{-3}$ )	$^{214}\text{Pb}^a$ ( $\text{Bqm}^{-3}$ )	$^{214}\text{Pb}^f$ ( $\text{Bqm}^{-3}$ )	$^{214}\text{Bi}^a$ ( $\text{Bqm}^{-3}$ )	$Z$ ( $10^3\text{cm}^{-3}$ )	$f_p$	F	No. of Values
February 1986	14.6 (4.2-37.7)	6.8 (1.4-21.5)	0.8 (0.0-3.0)	7.5 (1.9-24.1)	0.1 (0.0-1.6)	8.1 (2.0-22.4)	41. (14.-71.)	0.012 (0.0-0.098)	0.51 (0.37-0.67)	8
October 1986	11.3 (2.0-23.6)	7.8 (0.8-18.2)	1.5 (0.0-5.6)	8.4 (1.1-17.6)	0.2 (0.0-1.7)	9.1 (0.8-20.6)	41. (7.5-89.)	0.031 (0.0-0.180)	0.79 (0.51-1.15)	13
July 1988	6.9 (1.0-17.2)	3.9 (0.4-19.7)	0.6 (0.0-1.9)	4.3 (0.6-20.6)	0.1 (0.0-2.0)	4.6 (0.6-20.1)	23. (7.7-93.)	0.014 (0.0-0.216)	0.64 (0.23-1.19)	15
Mean	10.2 (1.0-37.7)	6.0 (0.4-21.5)	1.0 (0.0-5.6)	6.5 (0.6-24.1)	0.1 (0.0-2.0)	7.0 (0.6-22.4)	34. (7.5-93.)	0.020 (0.0-0.216)	0.67 (0.23-1.19)	36

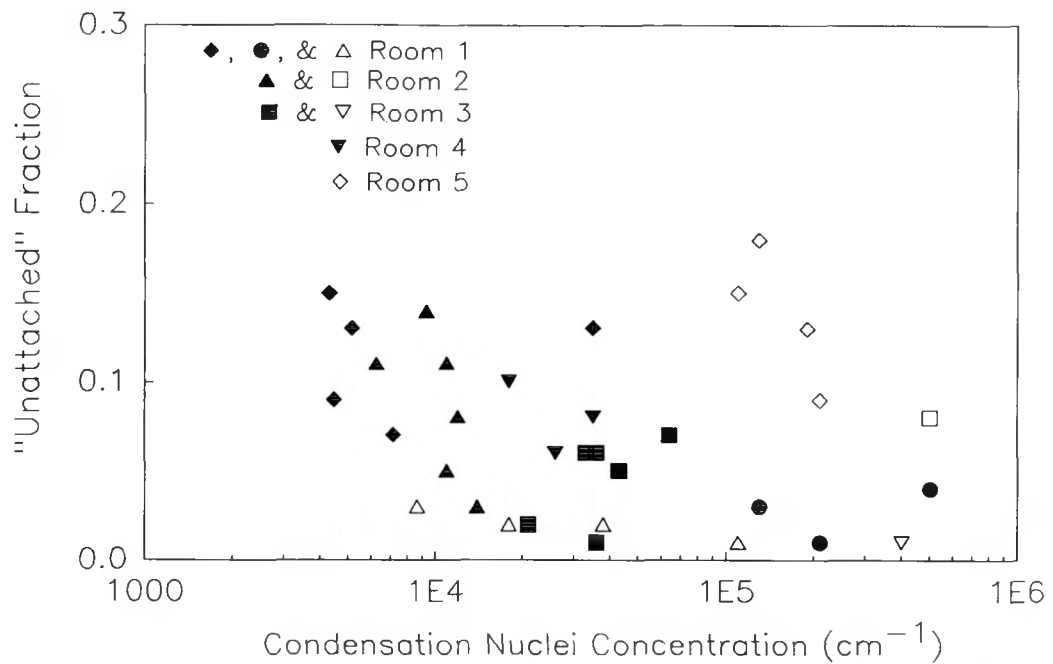


Figure 17. "Unattached" fraction of potential alpha energy concentration,  $f_p$ , as a function of the condensation nuclei concentration. Data taken from Porstendörfer (1987).

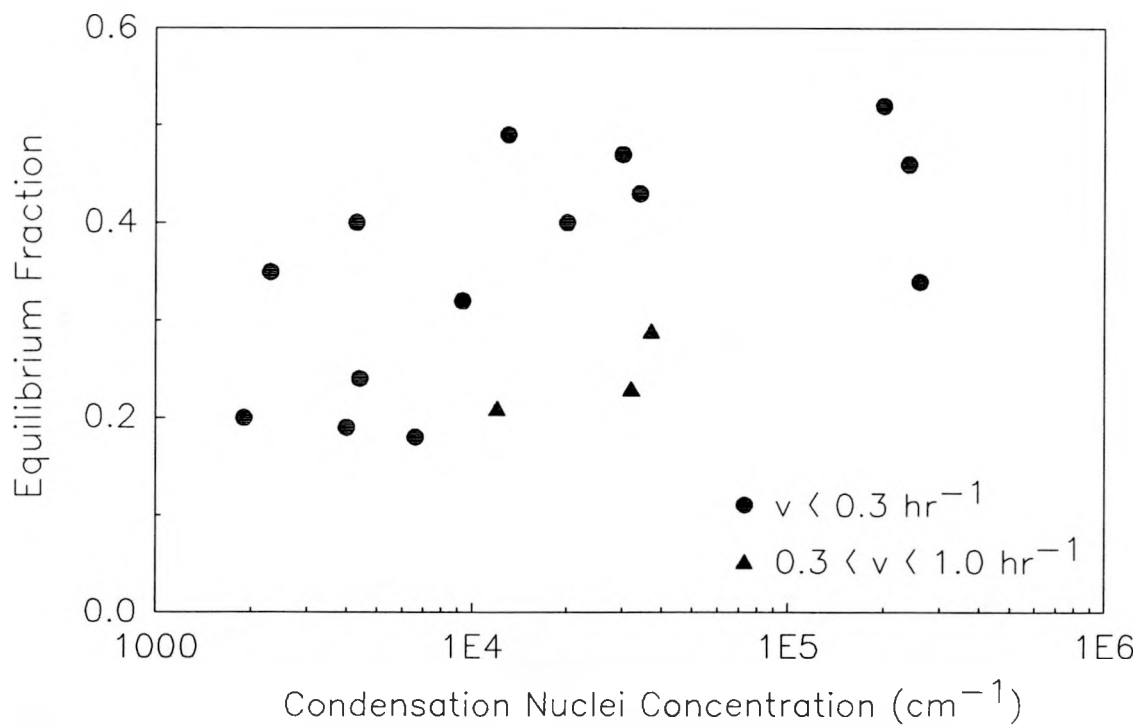


Figure 18. Equilibrium factor as a function of condensation nuclei concentration. Data taken from Porstendörfer (1987).

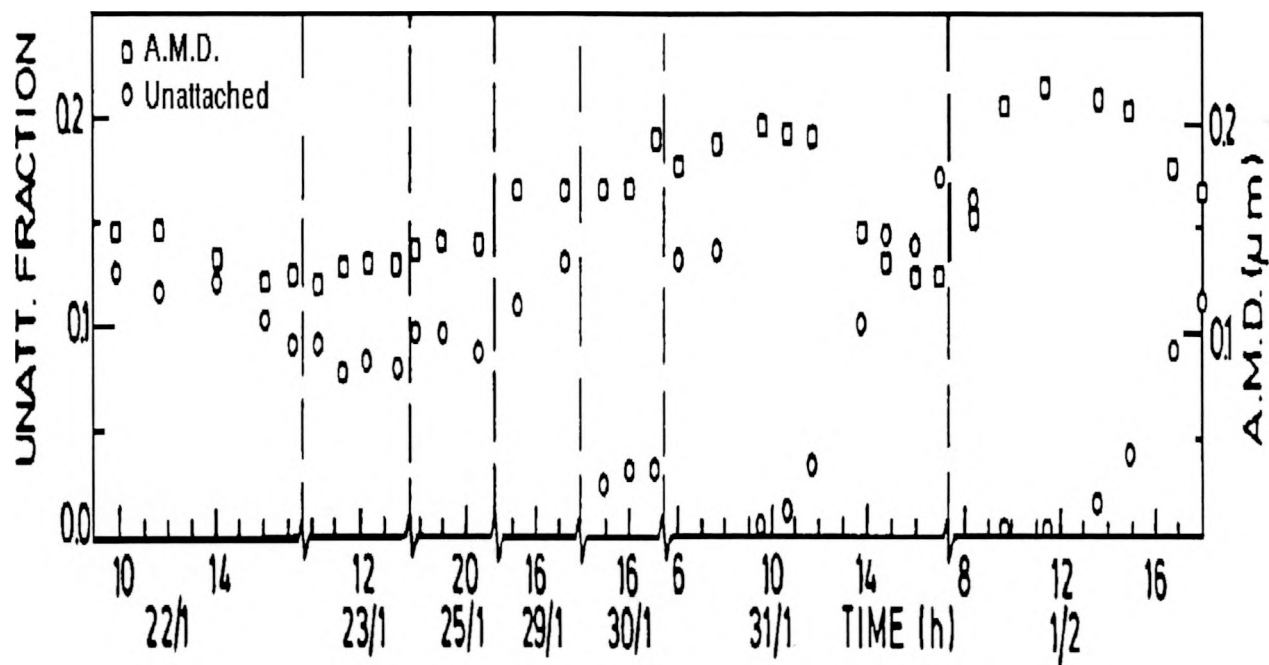


Figure 19. Time sequence of measurements in a Belgian house. Figure taken from Vanmarcke *et al.* (1985) and used with permission.

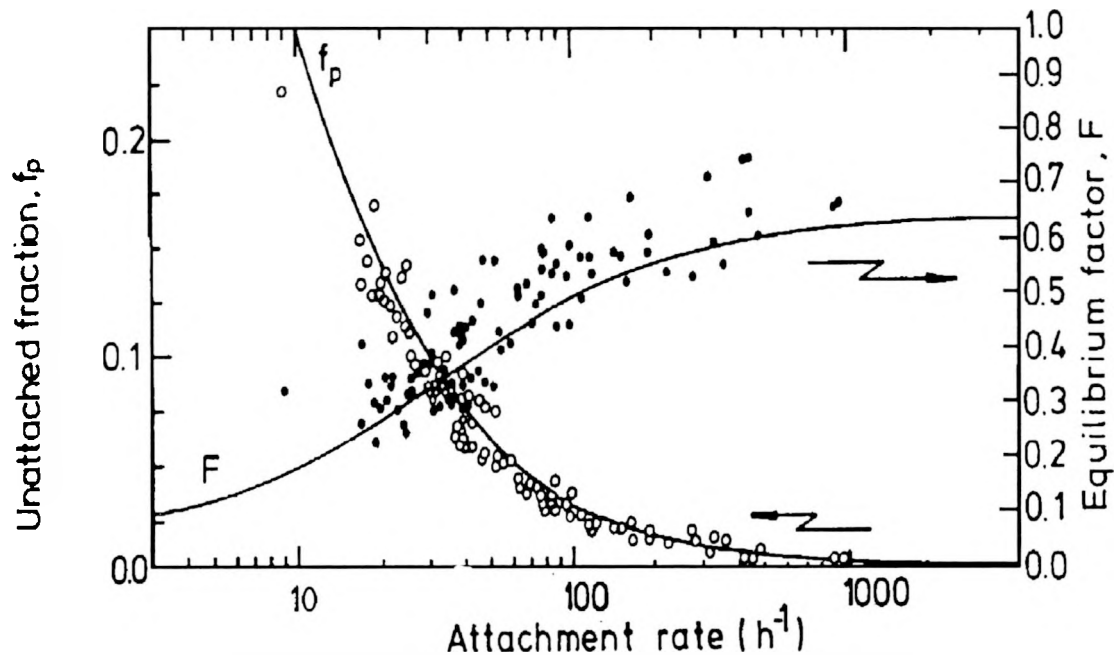


Figure 20. Equilibrium factor and the "unattached" fraction of potential alpha energy concentration as a function of the estimated attachment rate based on measured aerosol size distributions.

none of the publications by this group provide actual values of these variables nor summary statistics of their measurements.

The Gent group (Vanmarcke and coworkers) has intercompared their measurement methodology with the group from Göttingen (Reineking and Porstendorfer). The results of this intercomparison study have been presented by Vanmarcke *et al.* (1988). The results of the intercomparison of radon and radon decay product concentrations are presented in Figure 21. It should be noted that Gent values for  $^{218}\text{Po}$  are consistently higher than the Göttingen values while their radon concentrations vary between higher and lower values. There thus appears to be a consistent measurement problem that leads to high  $^{218}\text{Po}$  results and systematically high  $f_p$  values as shown in Figure 22. It can be seen that the Gent values are generally higher than the Göttingen values particularly in the absence of an additional aerosol source. The Göttingen unattached fraction values are generally in good agreement with those observed in other studies. Thus, although there is excellent agreement for their equilibrium fraction results, it appears that the Vanmarcke  $f_p$  values are high and may overestimate the true value by greater than 50%.

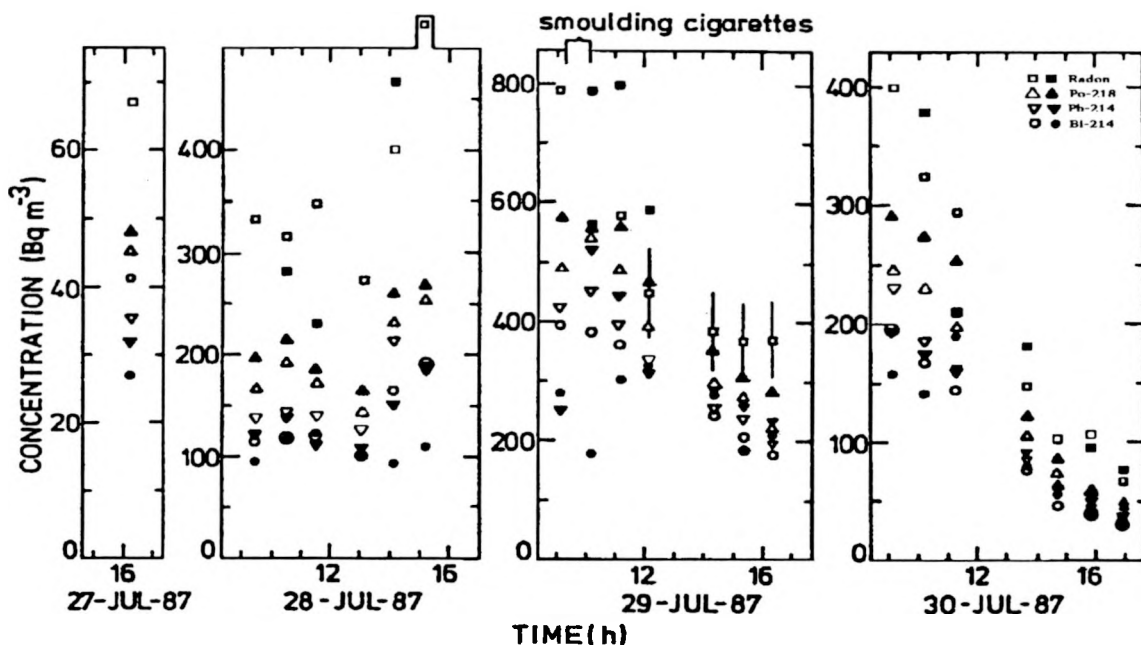


Figure 21. Radon and radon decay product concentrations measured during the Gent-Göttingen intercomparison study. Filled symbols are Gent; Open symbols are Göttingen. Figure taken from Vanmarcke *et al.* (1988) and used with permission.

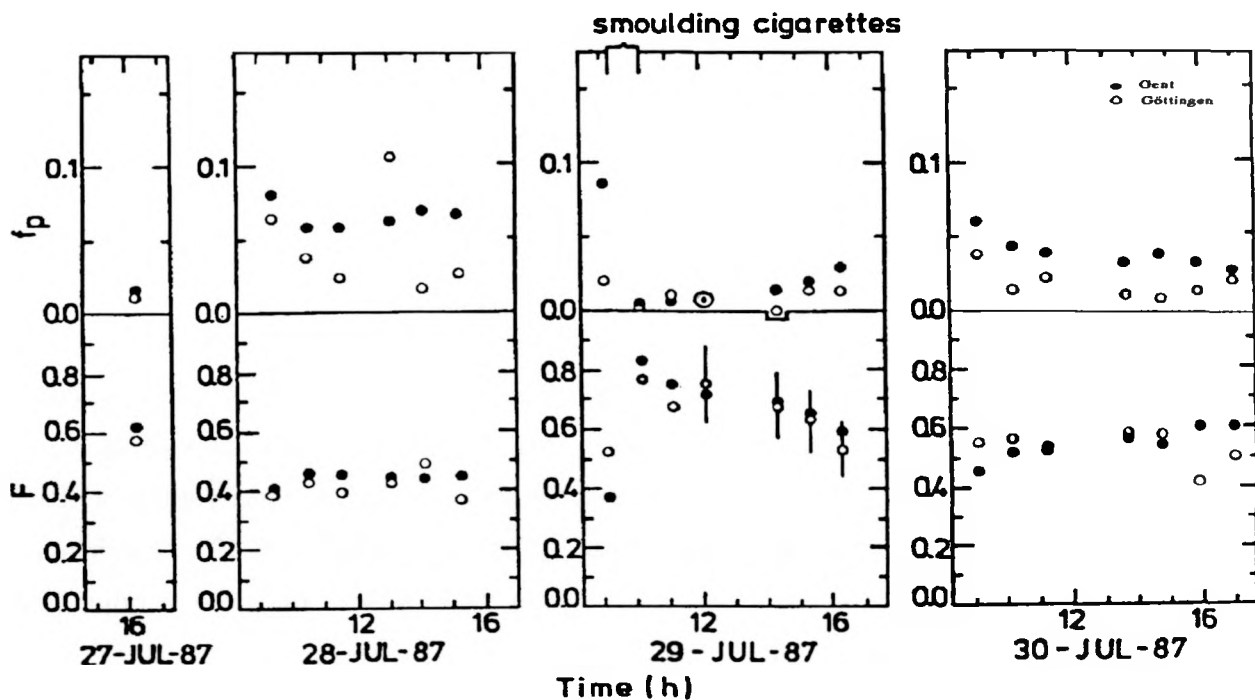


Figure 22. Evolution of the "unattached" and equilibrium fractions as measured in the Gent-Göttingen intercomparison study. Figure taken from Vanmarcke *et al.* (1988) and used with permission.

Stranden and Strand (1986) measured the "unattached" fraction and the equilibrium factor in occupied dwellings and an underground hydro-electric generating station and compared these results to their underground mining results. There are no descriptions of the housing units, the locations in which sampling occurred, nor the "normal activities" that were on-going in the dwellings and the generating station. They fit their data to an equation of the form

$$f_p = aF^b \quad (15)$$

where  $a$  and  $b$  are empirical coefficients. They linearize the equation using a logarithmic transformation and perform least-squares fits to the data. Such a process will produce a biased results because the uncertainties are not uniform and do not propagate linearly through a logarithmic transformation. The results they obtain are as follows:

Dwellings:  $f_p = 0.0172F^{2.34}$

Hydro-electric station:  $f_p = 0.0455F^{1.23}$

Mine:  $f_p = 0.016F^{1.12}$

If the same analysis is applied to the data obtained by Reineking and coworkers (1985; 1990), an equation of the form,  $f_p = 0.0177F^{-2.50}$  with a correlation coefficient of 0.80, is obtained. Thus, quite close agreement has been obtained for these different indoor spaces. These results indicate that the size distribution of the indoor aerosol must be similar in these houses although the concentration may vary.

Kojima and Abe (1988) have developed an automated tape sampler for the  $\alpha$ -spectroscopic measurement of the time sequence of "unattached" fraction in Japanese houses. They use a 500 mesh screen at a face velocity of  $29.7 \text{ cm s}^{-1}$ . They also use the Thomas and Hinchliffe calibration curve to estimate a collection efficiency of 99%. They calibrated the counting efficiency of activity on the screen. The correction factor for undetectable activity on the back of the screen was determined to be  $0.79 \pm 0.21$ . As in the other measurements of the front-to-back ratio (Holub and Knutson, 1987), the amount of activity on the back side of the filter is dependent on the actual size of the "unattached" mode. There is also a loss of activity in the sampler's inlet. The correction factor for the sampler head loss is  $0.82 \pm 0.10$ . They were able to measure  $2 \text{ Bq m}^{-3}$  of  $^{218}\text{Po}$  and  $0.3 \text{ Bq m}^{-3}$  of  $^{214}\text{Pb}$  with a relative standard deviation of 50%.

The instrument was then deployed in a detached, two-story concrete house with typical Japanese life style use. Figure 23 provides the diurnal variations of the "unattached" fractions of each of the three decay products and the aerosol concentration. The summary of "unattached" fraction measurements made over 7 months (November 1986 to May 1987) are presented in Table 5. It should be noted that during this 7 month period the total  $^{218}\text{Po}$  concentration drops from  $11.1 \text{ Bq m}^{-3}$  in November to  $3.9 \text{ Bq m}^{-3}$  in May. Thus, concentrations in this house are very low and Japanese construction and life style are quite different from that in the United States.

### Conclusions

"Unattached" fraction wire screen measurements must be tempered with the recognition that a) the "unattached" fraction is in reality an ultrafine cluster mode in the 0.5-3 nm size range, b) the collection efficiency versus particle diameter characteristics for wire screens do not allow a distinct separation of the "unattached" and "attached" fractions, and c) there can be collection of large particles ( $> 100 \text{ nm}$ ) on screens through inertial impaction (Reineking and

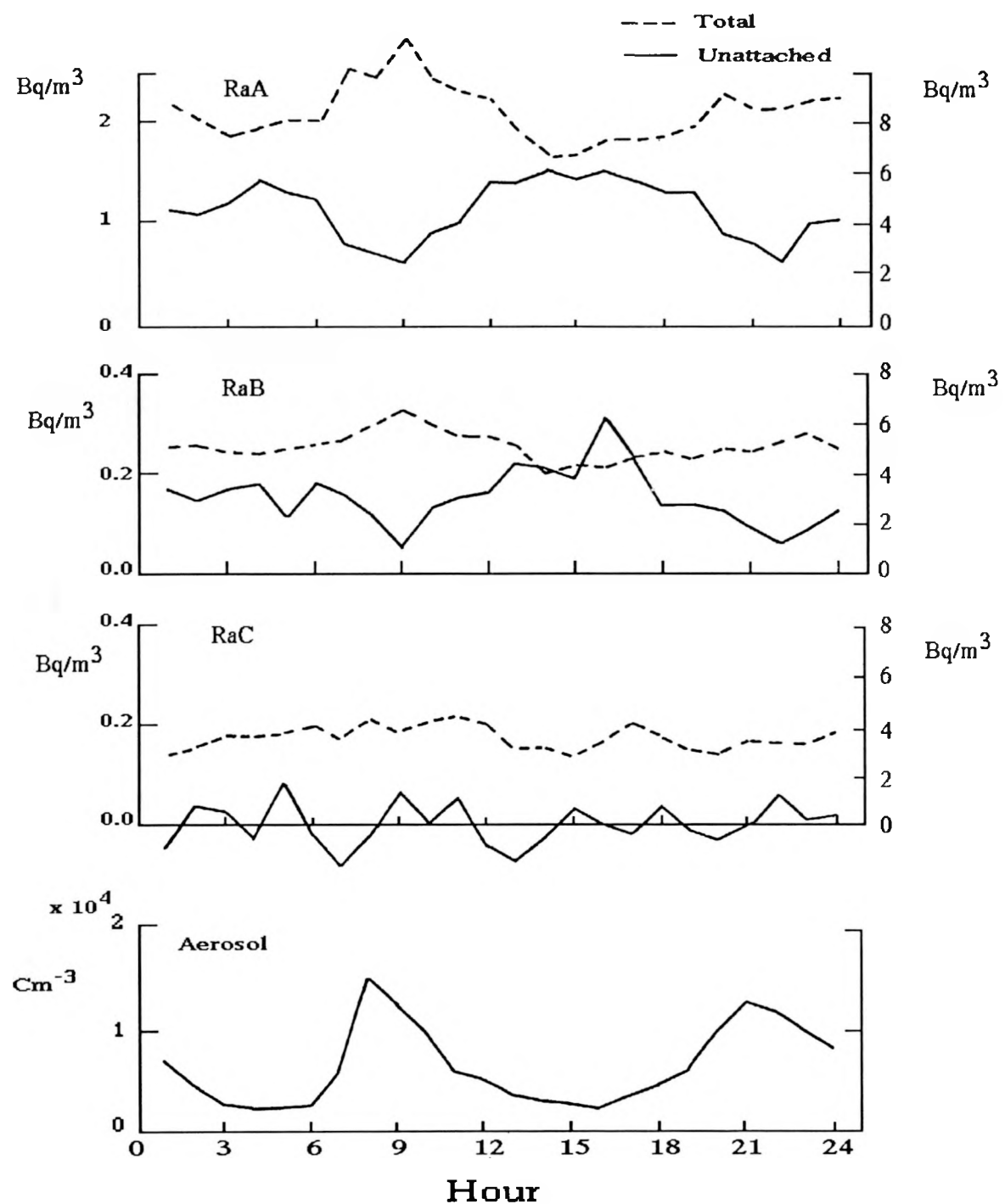


Figure 23. Diurnal variation of the "unattached" fractions of each of the radon decay products and the aerosol concentration. Left axis for Unattached; right axis for Total. Figure taken from Kojima and Abe (1988) and used with permission.

Porstendorfer, 1990). Through appropriate choice of screen operating parameters, efficient collection of the 0.5-3 nm activity fraction may be obtained, while minimizing the collection of "attached" activity. Reineking and Porstendorfer (1990) suggest an approach for correcting the measured "unattached" fractions of  $^{218}\text{Po}$  and  $^{214}\text{Pb}$  by assuming that in normal indoor aerosol particle concentrations ( $> 1000 \text{ cm}^{-3}$ ), all of the  $^{214}\text{Bi}$  is "attached." Thus, any apparent "unattached"  $^{214}\text{Bi}$  is really inertially collected larger particles. Then a correction can be made assuming that the "attached" size distributions for  $^{218}\text{Po}$  and  $^{214}\text{Pb}$  are the same as that of  $^{214}\text{Bi}$ . The "unattached" concentrations are then given by

$$c_j^f = c_j - \frac{c_c}{c_c - c_{c,sc}} (c_j - c_{j,sc}) \quad (16)$$

where  $c_j$  is the total activity of either  $^{218}\text{Po}$  or  $^{214}\text{Pb}$ , and the subscript sc denotes that activity deposited on the screen.

In general it appears that the "unattached" fraction of potential alpha energy concentration measured in active working areas of uranium mines are lower than in "typical" indoor air. It appears that the "unattached" fraction values in mines are approximately 3 times

Table 5. Summary results of the "unattached" fractions measured in a single Japanese house (Kojima and Abe, 1988).

Period	No. of Values	"Unattached" $^{218}\text{Po}$ $^{214}\text{Pb}$		"Unattached" PAEC
Nov. 1986	142	0.12	0.025	0.032
Dec.	168	0.11	0.028	0.034
Jan. 1987	144	0.12	0.035	0.043
Feb.	240	0.078	0.024	0.031
March	200	0.13	0.029	0.045
April	190	0.19	0.041	0.055
May	227	0.21	0.040	0.064

smaller than those measured in houses. The more recent measurements also suggest that the equilibrium factor in houses without smokers is lower than the commonly used value of 0.5 and is probably in the range of 0.30 to 0.40. Thus, although there is less airborne activity in indoor air per unit radon activity concentration, more of it is in the more diffusive form. However, there are relative few measurements of the behavior of radon progeny in houses under normal occupied living conditions over a prolonged period of time. The only such measurements are those of Kojima and Abe (1988), and the house and life style examined does not correspond to conditions in the United States. Thus, there is a need for much better information on the size distributions of the activity in the atmospheres of occupied houses in the United States.

To better define the actual behavior of the airborne activity, multiple wire screens can be used in diffusion battery-type systems to comprehensively determine the activity size distribution in the 0.5 - 500 nm size range as described by Reineking and Porstendorfer (1986), Kulju *et al.* (1986), Tu and Knutson (1988a), Strong (1988), Ramamurthi and Hopke (1990a), and others. These measurements will be discussed in the next section of this report.

## ACTIVITY-WEIGHTED SIZE DISTRIBUTIONS

Although the focus of this report is on "unattached" fractions, it is important to note that methods have been developed by which the entire radioactive aerosol size distribution can be deduced from data regarding the collection of activity on or its penetration through a series of screens. From these distributions, that portion of the size range that is to be defined as "unattached" can be calculated. Early measurements of the activity-weighted size distributions were made with conventional aerosol sampling systems such as tube or screen diffusion batteries (George and Breslin, 1980). Since condensation nuclei counters are commonly used as the particle detector for the corresponding number distributions, their rapid decrease in counting efficiency below 10 nm limits their utility to particle diameters  $> 5$  nm. Thus, these systems were typically designed with a minimum size "particle" of 10 nm in mind.

The first activity size measurements in indoor and ambient air were made by Sinclair *et al.* (1977) using a specially designed high volume flow diffusion battery. They observed bimodal distributions with activity mode diameters of 7.5 and 150 nm in indoor atmospheres and 30 and 500 nm outdoors in New York City. Similar results were reported by George and Breslin

(1980). Becker *et al.* (1984) only observed the larger mode using a modified impactor method with a minimum detectable size of 10 nm. Their measurements were made in Göttingen, West Germany. More extensive measurements in New York City by the group at the Environmental Measurements Laboratory (EML) have been reported by Knutson *et al.* (1984) using several different types of diffusion batteries as well as cascade impactors. They again observe modes around 10 nm and 130 nm in the PAEC-weighted size distribution measured with a low volume screen diffusion battery. Four samples taken with a medium volume (25 L min<sup>-1</sup>) screen diffusion battery showed a major mode at 80 to 110 nm and a minor mode containing 8 to 9% of the PAEC with a diameter < 5 nm. Finally, the same group made measurements at Socorro, NM (George *et al.*, 1984). They report that the major mode was only slightly different from that found in New York, but the minor mode was always < 5 nm, distinctly smaller than the New York distributions.

One of the problems with the extension of screen diffusion batteries to smaller particle sizes is the substantial collection efficiency of the high mesh number screens typically used in diffusion batteries designed to cover the range of particles size from 5 to 500 nm. At normally used flow rates, a single 635 mesh screen has greater than 90% efficiency for collecting 1 nm particles, the size of "unattached" <sup>218</sup>Po having a diffusion coefficient of the order of 0.05 cm<sup>2</sup>s<sup>-1</sup>. Thus, once the Yeh-Cheng screen penetration theory had been validated to 4 nm by Scheibel and Porstendorfer (1984) and the limitations of high mesh number screens were recognized, it was then possible to begin to examine alternative diffusion battery designs that could be extended to smaller particle diameters.

Reineking *et al.* (1985), Reineking and Porstendorfer (1986), Reineking *et al.* (1988) use the high volume flow diffusion batteries described in Reineking and Porstendorfer (1986) to obtain activity size distributions. They obtain their size distributions by fitting log-normal distributions using a SIMPLEX algorithm. Size distributions of indoor air in rooms without and with additional aerosol sources are presented in Figures 24 and 25. From these results, it would be surmised that the "unattached" fraction is the mode with median diameter 1.2 nm and geometric standard deviation of 1.5.

Holub and Knutson (1987) report the development of low flow diffusion batteries with low mesh number screens and extension of the EML batteries to smaller sizes. Tu and Knutson (1988a & b) have used the 25 L min<sup>-1</sup> screen diffusion batteries to measure the <sup>218</sup>Po-weighted

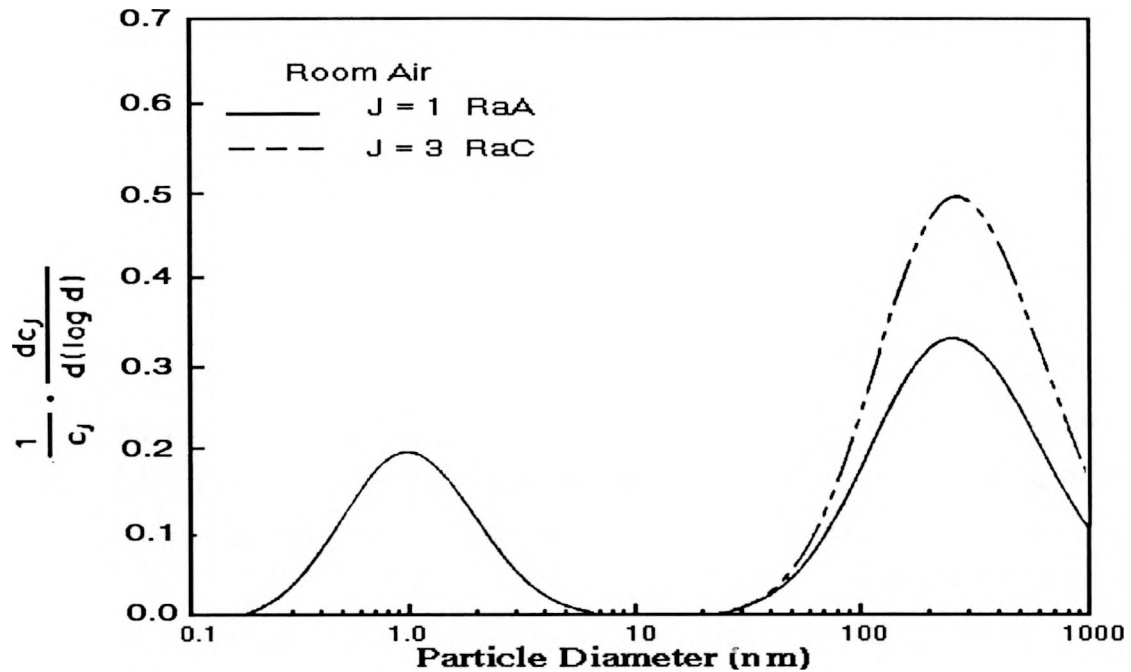


Figure 24. Activity-weighted size distribution of the indoor aerosol in a closed room without additional aerosol sources. Figure taken from Reineking and Porstendörfer (1986) and used with permission.

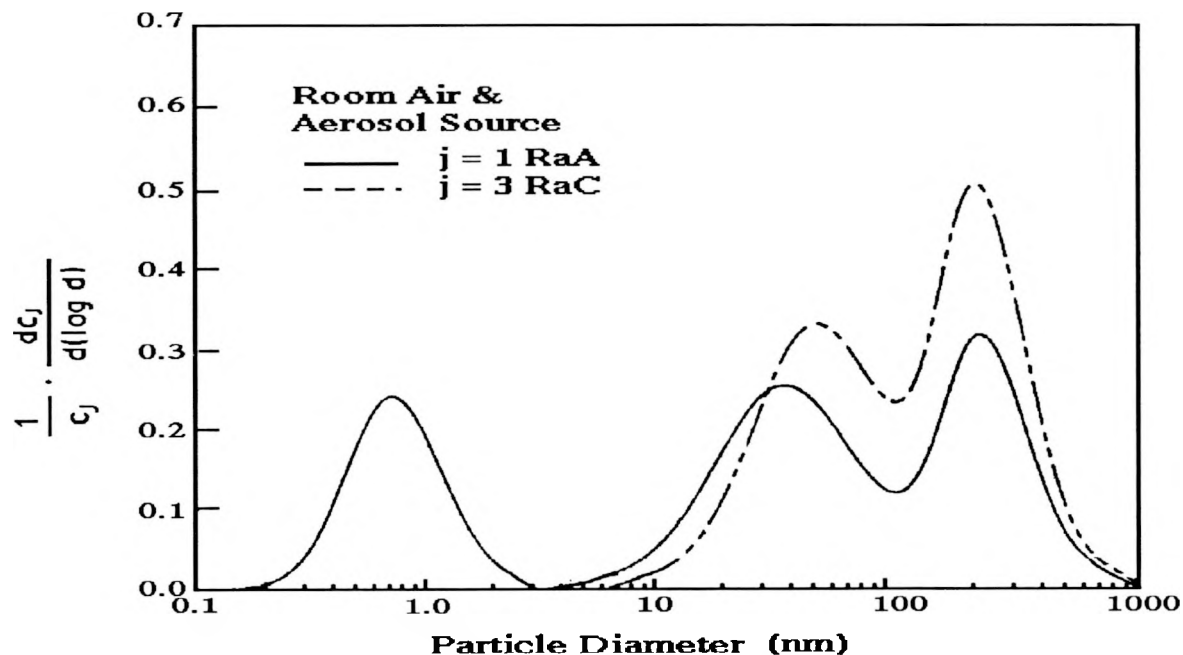


Figure 25. Activity-weighted size distribution of the indoor aerosol in a closed room with an additional aerosol source. Figure taken from Reineking and Porstendörfer (1986) and used with permission.

size distributions in the presence of several specific aerosol sources. The results of these measurements are presented in Figures 26 and 27. The presence of a mode around 10 nm is again observed in curve 1 in Figure 26. Only in curve 1 (no active aerosol sources) in Figure 27 is a mode at 1 nm observed. In all of the other cases, the activity is attached to the aerosol present in the house. The attachment was confirmed by independently measuring the aerosol size distributions using an electrical aerosol analyzer (Liu and Pui, 1975) and the attachment coefficients recommended by Porstendorfer *et al.* (1979). The agreement between the measured and calculated activity weighted size distributions were excellent.

Several other groups including the National Radiation Protection Board (NRPB) of the United Kingdom and the Australian Radiation Laboratory (ARL) have also developed these graded screen diffusion batteries for activity size distribution measurements. An intercomparison between these three groups (EML, NRPB, and ARL) has been performed (Knutson *et al.*, 1988). This initial comparison found difficulties for particles having size  $> 500$  nm and  $< 20$  nm. For the large particles, the problem arises from impaction on the screen and thus there is

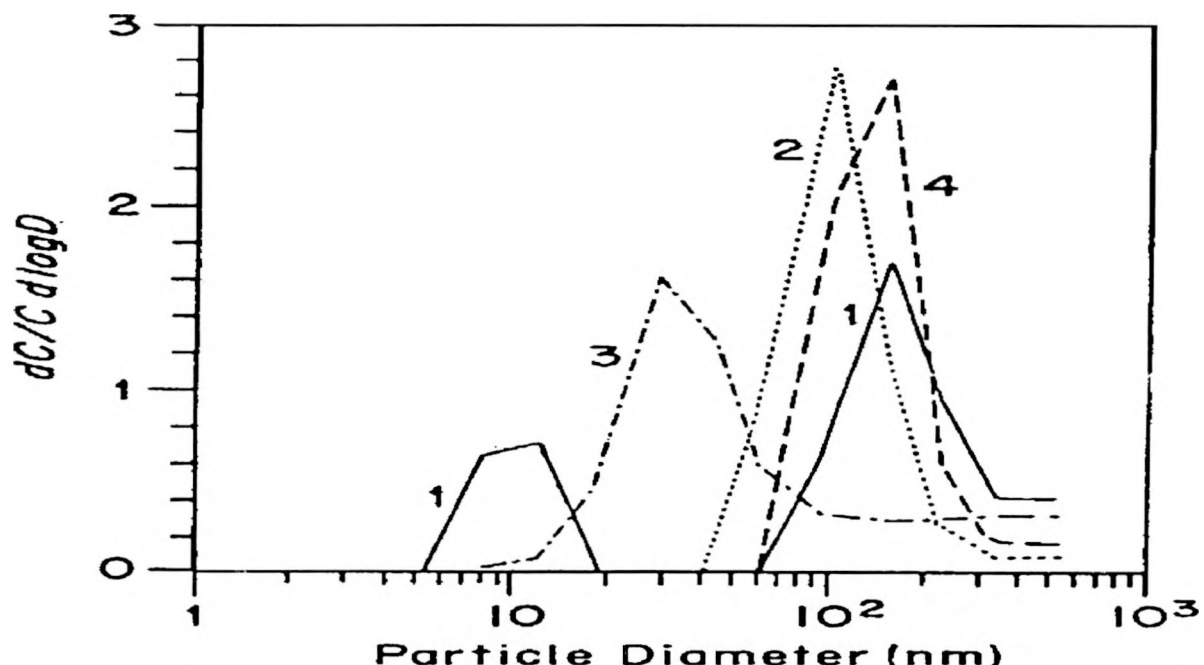


Figure 26.  $^{218}\text{Po}$ -weighted size distributions measured in house I. 1. cooking (5 min.); 2. frying food; 3. cooking soup; 4. cigarette smoldering. Figure taken from Tu and Knutson (1988a) and used with permission.

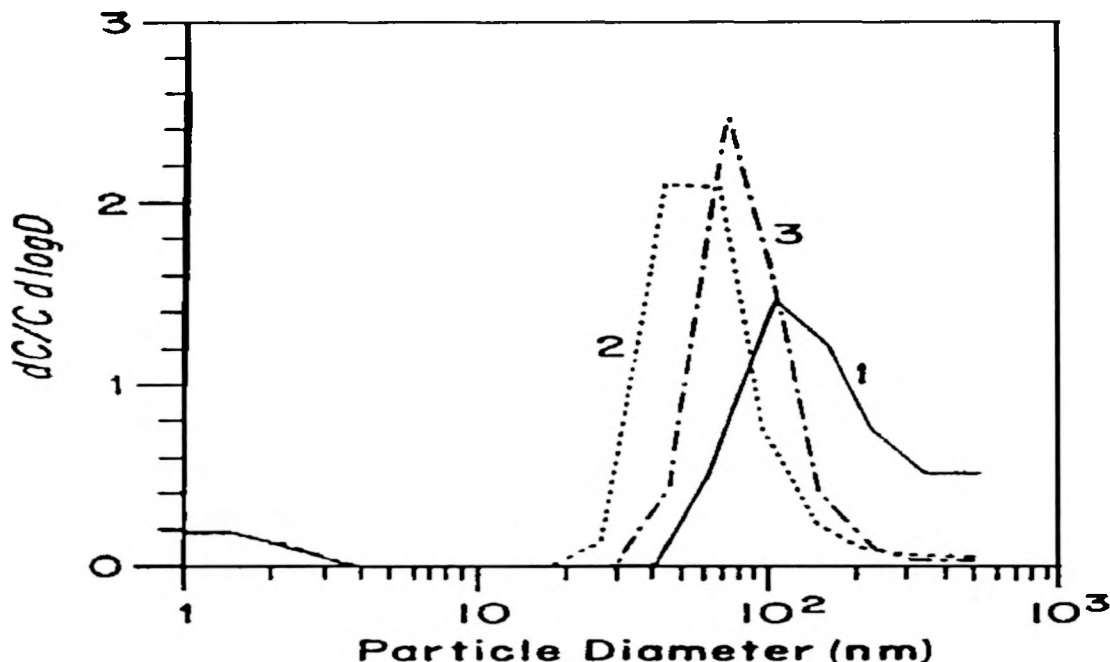


Figure 27.  $^{218}\text{Po}$ -weighted size distributions measured in house II after a kerosene heater was operated for: 1. 0 min; 2. 80 min; 3. 200 min. Figure taken from Tu and Knutson (1988a) and used with permission.

an apparently excessive collection of activity in the ultrafine size range. For the smaller particle size range, there were several unexplainable discrepancies among the measurements.

Further tests of the single screen methods were performed by Holub *et al.* (1988) in which EML, ARL, and the U.S. Bureau of Mines (BuMines) made measurements in a chamber at ARL. The results agreed well as to the size of the "unattached" progeny. There were differences of about a factor of two in the measured amounts of airborne activity, but these differences were attributed to differences in sampling location rather than difficulties with the various screen configurations. The single screen measurements showed significant differences from the conventional screen diffusion battery measurements for the "unattached" fraction size, but were in good agreement for the "attached" mode sizes. This results can be anticipated because of the lack of resolution for the diffusion battery below 5 nm.

Several more recent intercomparison studies involving these three groups, the US Bureau of Mines Denver Research Center (BuMines), Dr. P.K. Hopke's group (then at the University of Illinois) and the Inhalation Toxicology Research Institute at Albuquerque (ITRI) have found excellent agreement among the various activity weighted size measurements as well

as with the size distributions inferred from measurements of the particle size distribution using a differential mobility analyzer (Ramamurthi *et al.*, 1989). Thus, the results of these studies suggest it is now possible to measure activity-weighted size distributions from 0.5 to 500 nm.

Several automated systems to make use of this methodology have been developed. Strong (1988) using 6 sampling heads containing 0, 1, 3, 7 18, and 45 stainless steel, 400 mesh wire screens. He has measured the size distributions in several rooms in two houses at two times of the year. The size distributions observed in the kitchen are presented in Figure 28. These results are summarized in Table 6. It should be noted that in the "kitchen" curve in Figure 28, a trimodal distribution is observed; a true "unattached" fraction at 1 nm, a nuclei mode at 10 nm, and an accumulation mode at 100 to 130 nm. In the table, the "unattached" fractions presented are the integrated values from the size distributions. A problem then arises as to what "unattached" means since Strong integrates the distribution up to  $> 10$  nm to obtain that fraction that he attributes as being "unattached." For the kitchen with cooking distribution, the activity median diameter for the "unattached fraction is given as 11 nm. Such attribution is a clear departure from the original purpose for defining an "unattached" fraction. The advent of these measurement systems requires a more precise definition of the meaning of the "unattached" fraction.

Table 6. Summary of activity size measurements made by Strong (1988) in two houses in the United Kingdom.

Site	Ambient Aerosol			Attached		Unattached	
	Median (nm)	GSD	N (cm <sup>-3</sup> )	AMD (nm)	GSD	f <sub>p</sub> (%)	AMD (nm)
<b>Rural (summer)</b>							
Bedroom	42	2.0	5000	130	2.4	17	2.0
Living Room	30	2.0	5100	150	2.1	17	2.0
Kitchen	33	1.7	11000	130	2.0	18	6.0
Kitchen (cooking)	30	1.7	470000	110	1.9	11	11.0
<b>Rural (winter)</b>							
Living Room	32	1.7	4700	130	2.1	20	2.0
<b>Urban (winter)</b>							
Living Room	30	2.1	15000	110	2.1	20	3.5
Mean of all sites	33	2.0	8200	130	2.1	18	3.1

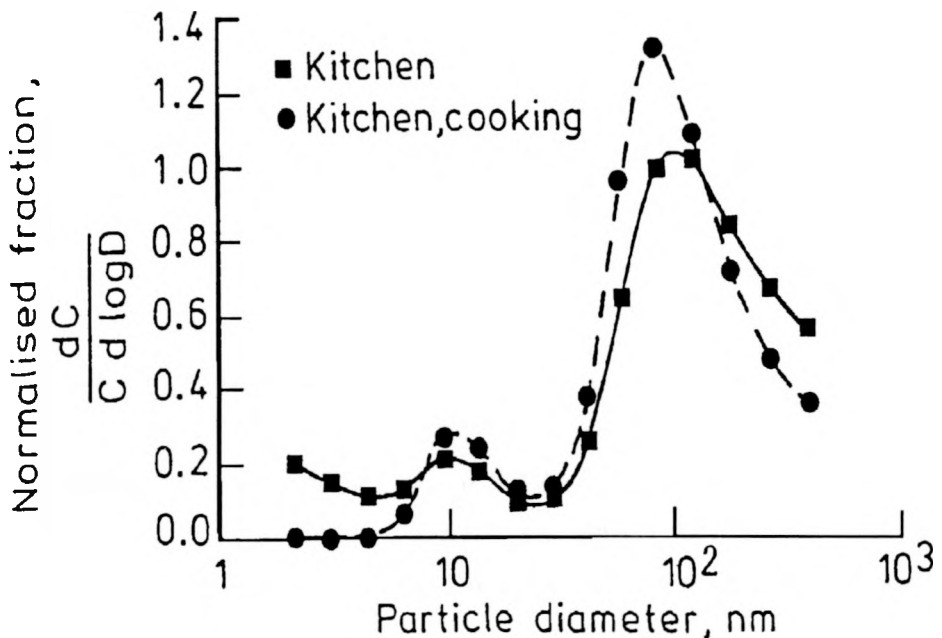


Figure 28. Activity size distributions measured in a rural house kitchen by Strong (1988). Used with permission.

Subsequent to these original measurements, Strong (1989) modified his system by changing the screens to 1 200-mesh screen and 1, 4, 14, and 45 400-mesh screens as well as the open channel. This modification provides a stage such that there is better resolution at the smallest sized particles such that the range of the system can be extended to 0.5 nm. The effective resolution cut-off of the original battery was about 2 nm. With the new battery, trimodal distributions are clearly observed (Figure 29). Although these measurements were made in the living room, the kitchen is adjacent and cooking with a gas stove was being performed at the time of these measurements. These results show the advantage of being able to measure the size distribution and determine the actual exposure of individuals to airborne radon progeny activity.

A similar system has been developed at the Australian Radiation Laboratory by Solomon (1989, personal communication). It is designed for measurements in the size range of 2 to 600 nm. The measurements have been extended to a smaller size range (0.5 to 100 nm) using a manual, serial single screen array sampling at 1 to 6  $\text{L min}^{-1}$  and to lower concentrations in the same size range using larger screens (9.5 cm diameter) and a 100  $\text{L min}^{-1}$  flow rate. Dr.

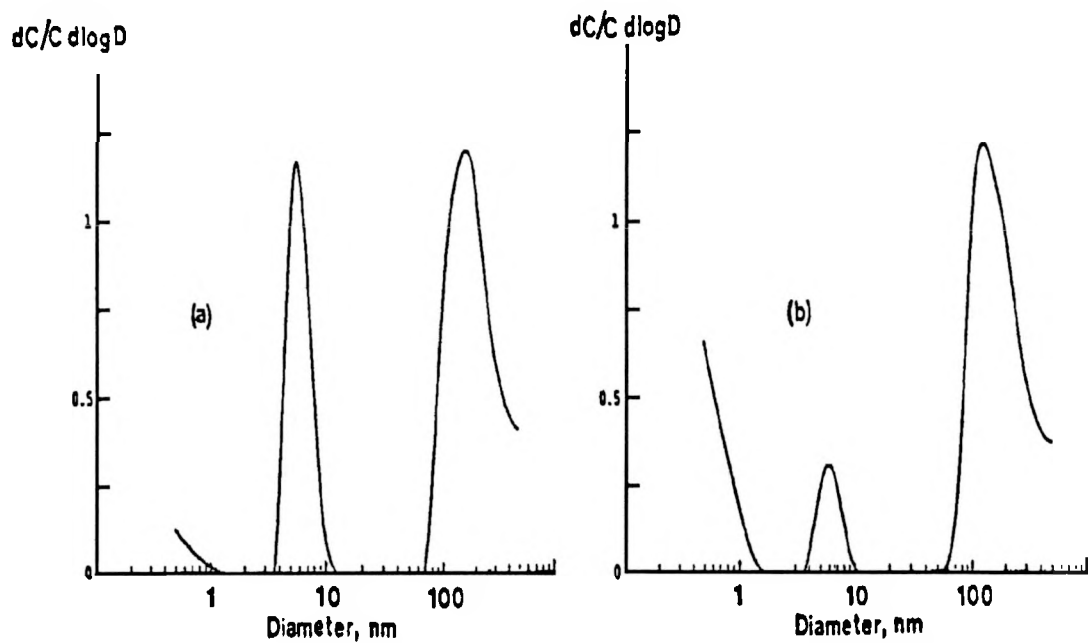


Figure 29. Tri-modal activity size distribution measured by Strong (1989) under conditions of a)  $F=0.36$ ,  $CN=10,000 \text{ cm}^{-3}$ ; b)  $F=0.26$ ,  $CN=5000 \text{ cm}^{-3}$ .

Solomon has examined both the Twomey (1975) and Expectation Maximization (Maher and Laird, 1985) algorithms for deconvoluting the size distributions from the screen penetration data. In both cases, he has developed a Monte Carlo method for determining the stability of the inferred size distributions. New input values for the concentrations found on each stage are chosen from a normal distributions using the measured radon decay product activity as the mean value and the measured uncertainty as the standard deviation of the distribution. This process can be repeated a number of times to provide a measure of the precision and robustness of the estimated size distributions.

A semi-continuous automated system has been developed at the University of Illinois by Ramamurthi and Hopke (1990a). This system consists of 6 sampling heads with various combinations of screens described in Table 7 along with their corresponding  $d_p(50\%)$  values. Activity size distributions were determined in a single house using this system. The measurements were conducted in a three-level residence in Princeton, NJ. The house (PU-22) is instrumented by the Center for Energy and Environmental Studies, Princeton University for continuous measurements of the radon concentration, temperature, humidity and differential

pressures. Activity size distributions were measured in the basement and first floor of the house over a 1 week period (9/13-9/20/89). Grab samples for decay product activity concentrations were taken intermittently and analyzed by the gross alpha-photomultiplier tube method for a comparison with the total concentration estimates from the automated system. The detectable particle number concentration in the sampling environment was continuously monitored by a Environment One Model 100 Condensation Nuclei Counter (CNC).

Initial activity size distribution measurements were made in the basement of the home. Number concentrations of particles in the basement varied between 2000-8000 cm<sup>-3</sup> as detected by the CNC. The lack of windows or other major openings to the outside is thought to be responsible for the low concentrations. Radon concentrations varied between 5-500 pCi/l during the seven day period with the time period for fluctuations being much longer than the 15 min sampling interval. A total of 15 measurements were made during the 7 day period with a remarkable degree of consistency in the shape of the measured activity size distributions. Figure 30 shows the typical Po-218, Pb-214, and Bi-214 distributions observed in the basement of the house at a radon concentration of 55 pCi/l and a particle number concentration of 3000 cm<sup>-3</sup>. The Po-218 distribution in Figure 30 is plotted as a histogram to illustrate the nature of the distribution while the Pb-214 and Bi-214 distributions are shown by curves connecting the mid-point diameter values.

Table 7. Assessment of measured screen penetration compared to theoretical predictions of Ingham (1975).

Unit	Sampler Slit Width (cm)	Sampler Diameter (cm)	Wire Screen* Mesh x turns	$d_p(50\%)$ (0.5-350nm range) (nm)
1	0.5	5.3	-	-
2	0.5	5.3	145	1.0
3	0.5	5.3	145 x 3	3.5
4	0.5	5.3	400 x 12	13.5
5	1.0	12.5	635 x 7	40.0
6	1.0	12.5	635 x 20	98.0

Sampling flow rate = 15 lpm (each unit)  
Detector-Filter separation  $\approx$  0.8 cm (all units)

\* Wire screen parameters given by Yeh et al. (1982).

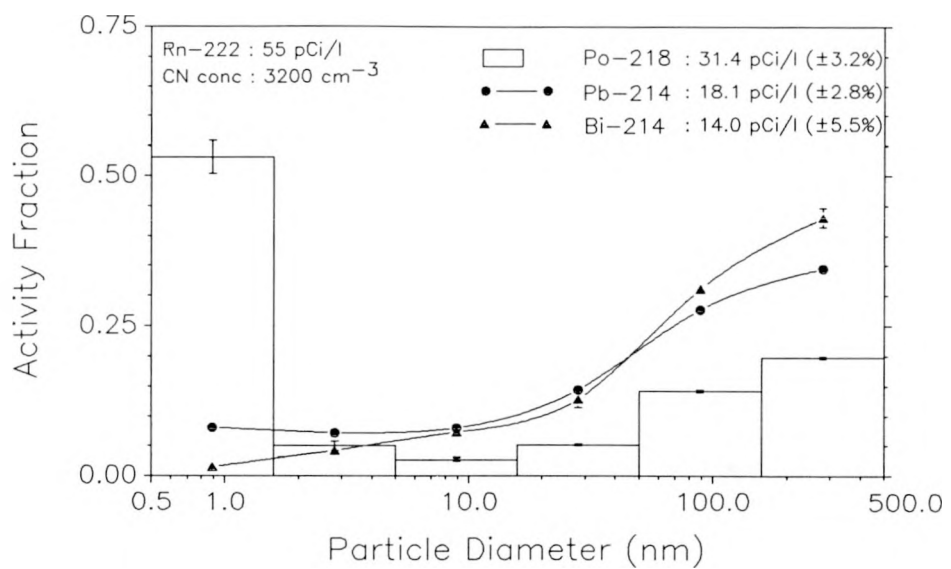


Figure 30. Typical Po-218, Pb-214, and Bi-214 activity size distributions observed in a house basement in Princeton, N.J.

The Po-218 distribution shows that  $\approx 54\%$  of the Po-218 activity is in the smallest inferred size interval with a mid-point diameter of  $\approx 0.9$  nm (diffusion coefficient,  $D \approx 0.04$  cm<sup>2</sup>/sec). This fraction closely resembles the classical, highly diffusive "unattached" fraction. The magnitude of the cluster fraction agrees well with theoretical predictions from attachment rate calculations at the observed particle number concentration (Porstendorfer *et al.*, 1979). Very little of the Po-218 activity exists in the range from 1.6 to 16 nm, with the remainder of the activity attached to the larger ambient aerosol particles, diameter  $> 50$  nm. The corresponding Pb-214 and Bi-214 distributions show much smaller activity fractions in the 0.9 nm size range. The longer lifetime of these decay products permits a greater fraction of activity to become attached to the ambient aerosol. For all three distributions, the "attached" mode peaked in the 160-500 nm size range. However, this measurement system cannot be used to determine particle sizes greater than 500 nm. The activity distributions obtained are in general agreement, both with respect to the Po-218 cluster fraction and the size range of "attached" activity, with the distributions measured by Tu *et al.* (1989) in the basement of this house under similar conditions at an earlier date.

Several measurements of activity size distributions were also made in the kitchen on the first level of the house. The initial measurements were performed under typical conditions of 20,000 particles/cm<sup>3</sup> and a radon concentration of  $\approx$ 3 pCi/l. The results of the measurement are shown in Figure 31. The Po-218 size distribution shows a large fraction of the Po-218 activity ( $\approx$ 44%) having a diffusivity similar to the classical "unattached" fraction. However, a significant fraction ( $\approx$ 10%) is in the 1.6-5.0 nm size interval. The corresponding Pb-214 and Bi-214 distributions indicate insignificant activity fractions in the 0.5 - 1.6 nm size interval, but a significant mode between 1.6 and 5.0 nm. The differences in the size distributions obtained in the basement and in the kitchen area relate primarily to the 1.6-5.0 nm size interval with the attached activity modes remaining in the 160-500 nm size range. This result suggests the presence of condensable constituents leading to the formation of particles in the 1.6-5.0 nm size interval or a source of very fine primary particles. This process may then allow the radon decay products to become associated with the 1.6-5.0 nm size mode in varying fractions depending upon the relative lifetimes. The presence of 6 large gas range pilot lights may be related to the formation of this mode, and similar effects are believed to have been observed in other houses by Tu *et al.* (1989).

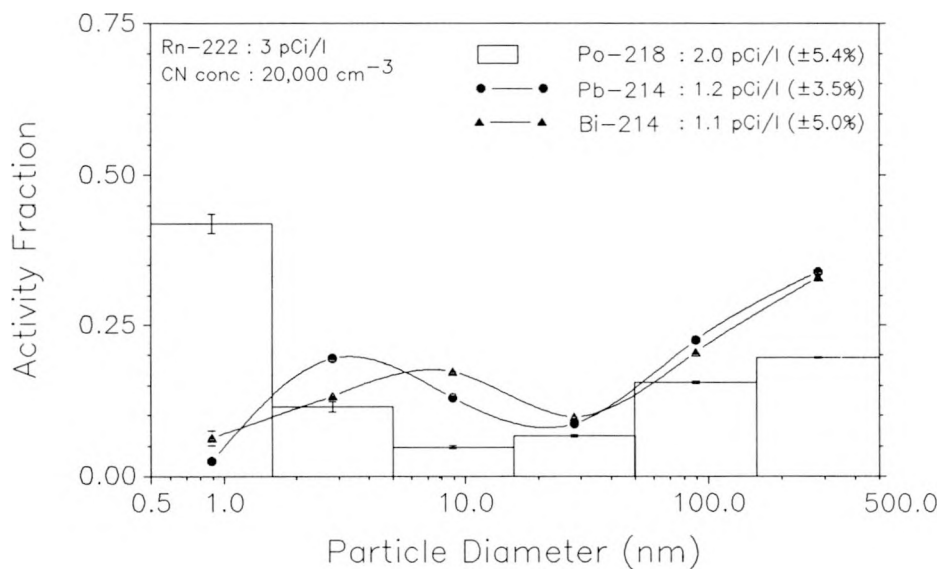


Figure 31. Po-218, Pb-214, and Bi-214 activity size distributions measured under typical conditions in the kitchen of the test house.

In a final experiment, activity size distributions were measured following the continuous addition of aerosols generated in the kitchen from lighting the gas stove burners of the kitchen range. Figure 32 shows the distributions measured with particle number concentrations of  $\approx 150,000 \text{ cm}^{-3}$  and a radon concentration of  $\approx 2 \text{ pCi/l}$ . The large concentrations of particles generated could be presumed to be rapidly coagulating soot cluster aggregates. The Po-218 and Pb-214 activity distributions measured under these conditions (Figure 32) are dramatically different from those measured in the basement and background kitchen conditions. The Po-218 distribution reveals very little activity in the 0.5 to 1.6 nm size interval ("unattached"), with most of the activity spread out over the range from 1.6 to 50 nm size intervals. The fraction of Po-218 attached to particles  $> 100 \text{ nm}$  is reduced to a negligible level, probably because of the very large number of smaller particles produced by the gas burners. The distribution of Pb-214 reveals the activity to be spread out over the size spectrum  $d_p > 1.6 \text{ nm}$ , while the Bi-214 distribution remains similar to those measured prior to the addition of external aerosols. However, these latter results may be due to the timing of the sampling interval, between 20-35 min after the start of continuous addition of the external aerosols. Consequently, steady-state Pb-214 and Bi-214 distributions may not have been attained.

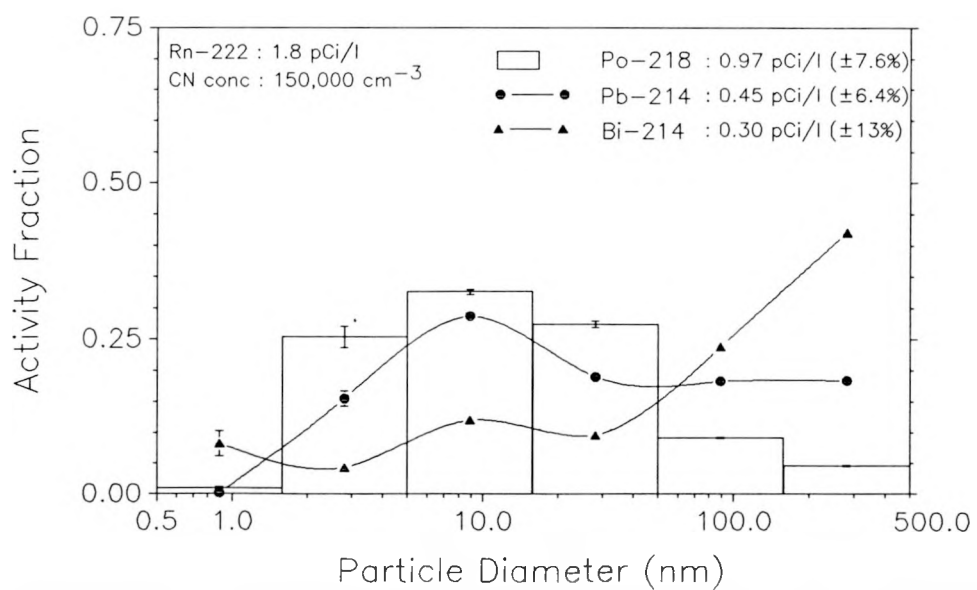


Figure 32. Po-218, Pb-214, and Bi-214 activity size distributions measured during the continuous generation of aerosols from the kitchen gas stove burners.

A stability analysis was performed for each of the size distributions shown in Figures 30, 31, and 32. This analysis provides an estimate of the stability of the inferred solutions with respect to errors in the input penetration data and the results are represented by the error bars indicated in the figures. The size distributions obtained in the experiments were found to be stable and relatively insensitive to perturbations in the input data of the order of the associated measurement errors. The errors in the size interval fractions estimated from this procedure are too small to be seen in these figures and thus were not included.

## **SAMPLER DESIGN BASED ON RESPIRATORY DEPOSITION**

### Introduction

From the discussion above, it should be clear that "unattached" fraction measurements have only limited value in assessing the actual size distribution of the radon progeny. It is now possible to measure the activity-weighted size distributions on a semi-continuous basis and more such studies are needed in order to develop and validate models from which population exposure estimates can be made. However, it would be useful if an alternative sampler could be devised that had the simplicity of measurement of a screen-type "unattached" fraction measurement, but could be more directly related to the deposition of activity in the human respiratory system and hence to the dose to the critical tissues. From the currently available information on respiratory tract behavior of particles, it appears feasible to devise such an alternative system. The information on respiratory tract deposition of particles and thus the basis for such a sampler will be presented along with the conceptual design of a new sampler to measure the "bronchial deposited" fraction of the radon progeny.

### Nasal Deposition

The critical questions in trying to assess the dose resulting from a given exposure to airborne  $^{22}\text{Rn}$  decay products is their fractional penetration through the nasal cavity. There is a lack of experimental data in the literature on nasal deposition. George and Breslin (1969) reported that between 28-50% of the "unattached" activity penetrated the nasal cavity during nose breathing while essentially all of the unattached activity penetrated to the respiratory tract during mouth breathing. These results are in agreement with the laboratory results of Schiller (1985) for particles  $\geq 5$  nm in diameter.

Based on a survey of the available experimental literature, Yu *et al.* (1981) have determined that oral deposition of micron-sized particles was less than for nasal deposition but was still appreciable. However, based on the analysis of the experimental systems used to measure total respiratory deposition by Gebhart *et al* (1989), Egan and Nixon (1989) have developed a corrected theoretical model to compare to Schiller's data. When simulating mouth breathing, they assumed that the oral deposition is zero and obtained excellent correspondence between theory and experiment over a range of particle sizes from 5 to 200 nm.

Recent improvements in airborne size measurements (Reineking and Porstendörfer, 1986; Holub and Knutson, 1987) have permitted the measurement of the size distribution of the airborne activity down to sizes below 1 nm. It appears from these measurements that the "unattached" fraction is an ultrafine mode in the activity size distribution whose exact size depends on the chemistry of the atmosphere in which the decay products are found (Hopke and Ramamurthi, 1988; Ramamurthi *et al.*, 1990b). The amount of activity penetrating the nasal cavity is thus dependent upon the size distribution of the radioactivity in the ultrafine-cluster size region.

Cheng *et al.* (1988) have presented the results of a new experimental study of the penetration of ultrafine particles (0.0046 to 0.2  $\mu\text{m}$  in diameter) through a nasal cast. A relationship between nasal deposition efficiency, inspiratory flow rate and particle diffusion coefficient was derived from the experimental data by Cheng *et al* (1988),

$$\eta = 1 - \exp(-40.3Q^{-1/8}D^{2/3}) \quad (17)$$

where  $\eta$  is the deposition efficiency,  $Q$  is the volumetric flow rate ( $1 \text{ min}^{-1}$ ), and  $D$  is the particle diffusion coefficient ( $\text{cm}^2 \text{ s}^{-1}$ ). The diffusion coefficient has been calculated using the modified Einstein-Cunningham equation presented earlier in this report. A plot of the fractional deposition in the nasal cavity as a function of particle size is presented in Figure 33, from a calculation using equation 17 and flow rates,  $Q$ , of 5 and 50  $1 \text{ min}^{-1}$ .

From the extrapolation of the previous data to the size of "unattached" radon progeny (about 1 nm), deposition efficiency is predicted to be greater than 90 % as shown in Figure 33 (Hopke *et al.*, 1990). Strong (personal communication, 1989) from National Radiological Protection Board (NRPB) of the United Kingdom found that the nasal deposition in a different half nasal cast followed a collection efficiency equation of  $\eta = 1 - \exp(-16 Q^{-1/8} D^{2/3})$ . Recently, the new empirical nasal deposition equation developed by Cheng (1989) is  $\eta = 1 -$

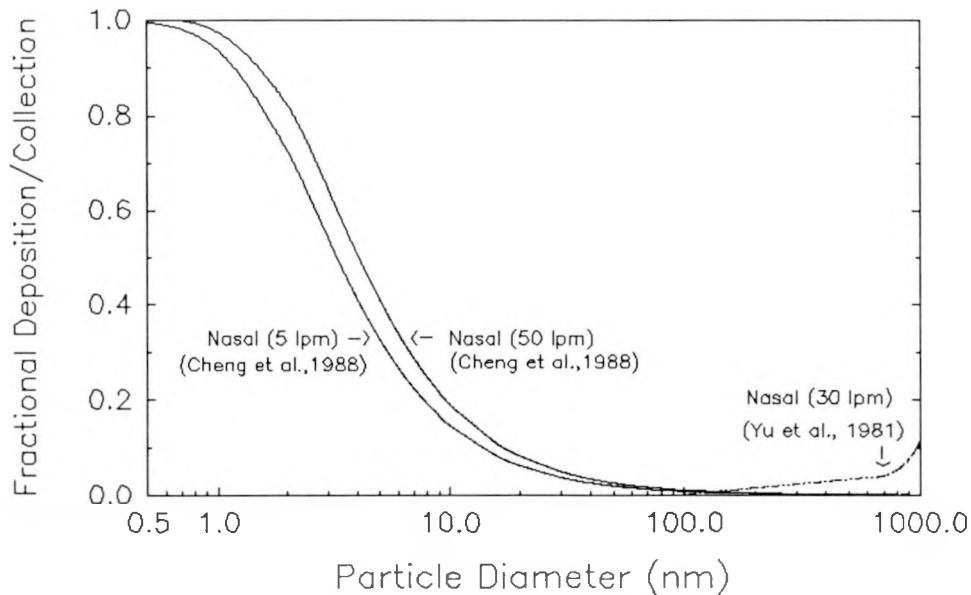


Figure 33. Fractional collection of particles in the nasal cavity as modeled by Equation 17.

$\exp(-12.3 Q^{1/8} D^{1/2})$ . Most recently, James *et al.* (1989) has reanalyzed the human nasal penetration data of George and Breslin (1969) and obtained the nasal deposition efficiency as  $\eta = 1 - \exp(-12.5 Q^{1/8} D^{2/3})$ . Thus, there is considerable uncertainty regarding the nasal penetration of the smallest sized radioactive particles. It would appear, however, that there is somewhat higher nasal deposition than has been typically incorporated into previous dosimetric models.

Yu and coworkers (Yu *et al.*, 1981; Yu and Diu, 1982) derived an empirical nasal inspiratory deposition efficiency relationship for larger particle sizes where inertial collection effects may become significant ( $d_p > \approx 200$  nm). Figure 33 also shows the fractional deposition in the nasal cavity calculated using these equations (Yu and Diu, 1982), using an inspiratory flow rate of 30 l min<sup>-1</sup> and assuming a particle density of 1 gm cm<sup>-3</sup>. It is evident from the calculated deposition curve shown in Figure 33 that under these conditions, the inertia-dominated, nasal deposition efficiencies are less than 10% for particle sizes  $\approx 1000$  nm (1  $\mu$ m).

#### Bronchial Deposition

The assessment of the lung alpha dose requires an estimate of the decay product activity deposited in the bronchial tree. It is possible to estimate the bronchial deposition as a function

of particle size in a manner similar to nasal deposition. Particle deposition in the bronchial tree in the size range  $d_p < 1 \mu\text{m}$  has been investigated by a number of researchers (e.g. Task Group on Lung Dynamics, 1966; Yeh and Schum, 1980; Yu *et al.*, 1981; Yu and Diu, 1982; Cohen *et al.*, 1990). The deposition in the bronchial region can be calculated using lung model parameters, empirical deposition relationships and correction factors developed in these and other reports.

The calculated fractional collection within the bronchial region is shown in Figure 34 at an average inspiration/expiration flow rate of  $30 \text{ l min}^{-1}$  and assuming particle densities of  $1 \text{ gm cm}^{-3}$ . The calculation estimates the collection of particles in the tracheobronchial region (generations 0-15) during both inhalation and exhalation, and is based on lung model parameters given by James (1984) and Yeh and Schum (1980). The deposition equations used in the calculation were those presented by Yu and Diu (1982) for laminar flow diffusional deposition, and deposition by impaction and sedimentation mechanisms. The correction factors determined experimentally by Cohen (1987) and Cohen *et al.* (1990) to correct for incomplete development of uniform laminar flow in generations 1-6 were also used in the calculation. The calculation

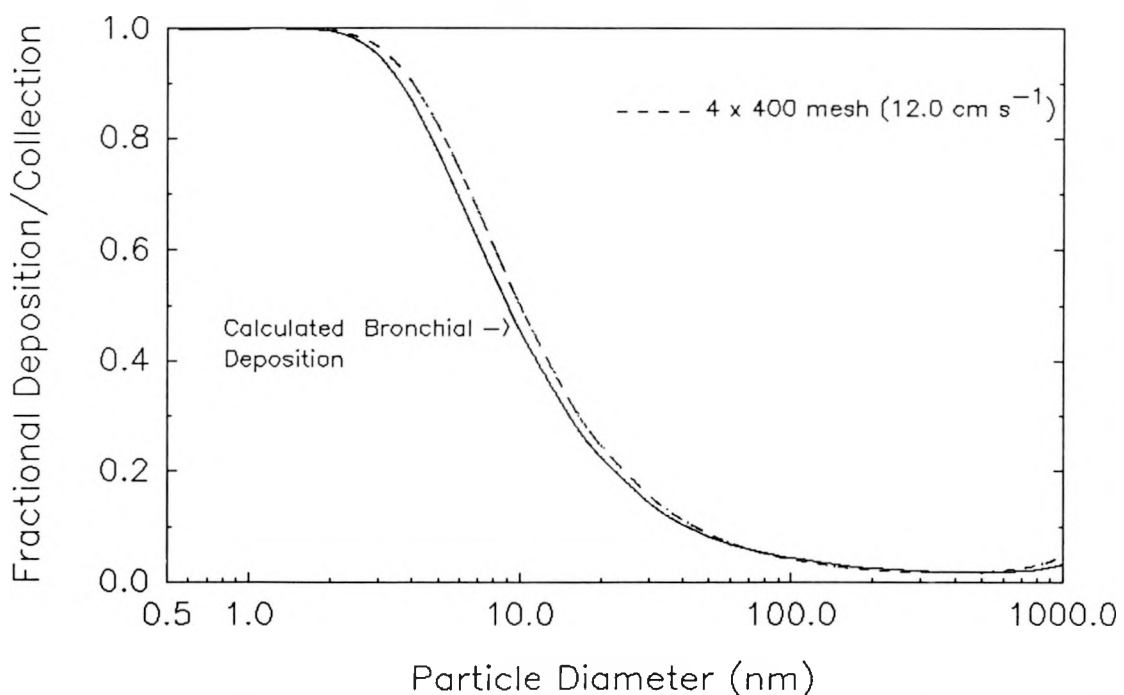


Figure 34. Fractional tracheobronchial deposition (generations 1-16) at  $30 \text{ l min}^{-1}$ . Also shown is the collection characteristic of four 400 mesh screens at a face velocity of  $12.0 \text{ cm s}^{-1}$ .

does not include corrections for dead volume in the trachea, assumes there is no pause between breaths, and that the air is inhaled completely into all generations of the lung. The calculated bronchial deposition curve is consistent with similarly calculated deposition curves presented by James (1988).

It is possible to select a multiple-wire screen sampler with similar collection characteristics as those of the bronchial region. In the case of an inspiratory/expiratory flow rate of  $30 \text{ l min}^{-1}$ , the collection efficiency of four 400-mesh screens with the same characteristic parameters as given previously and a face velocity of  $12.0 \text{ cm s}^{-1}$  provides an excellent match to the bronchial deposition pattern over the size range 0.5-1000 nm (Fig. 2). Thus, this wire screen measurement system would provide a good estimate of the sum of activity deposited in the bronchial region from both the "unattached" and "attached" modes.

### Sampler Design

It is now possible to design a sampling system that can provide measurements of airborne radioactivity from which the activity deposited in the nasal cavity or in the bronchial region can be estimated. The sampler would have several sampling heads depending on which quantities were to be determined. In each case, the activity collected on the filter would be counted using either a gross  $\alpha$  or  $\alpha$ -spectroscopy system to provide the data from which the activities of each of the decay products could be calculated. An open-faced filter would yield the total airborne activity ( $A_T$ ). A sampler with a single 400-mesh screen covering the filter and operating at a face velocity of  $12.0 \text{ cm s}^{-1}$  would give the amount of activity penetrating the nasal cavity for an inspiratory flow rate of  $30 \text{ l min}^{-1}$  ( $A_N$ ). The activity deposited in the nasal cavity is then given by  $A_T - A_N$ . From these quantities of deposited activity, the dose to the cell-at-risk could then be more accurately estimated.

A sampler with four 400-mesh screens covering the filter and also operating at a face velocity of  $12.0 \text{ cm s}^{-1}$  would measure the amount penetrating the bronchial region for a inspiratory/expiratory flow rate of  $30 \text{ l min}^{-1}$  ( $A_B$ ). If deposition in the oral passage during mouth breathing can be neglected, the activity deposited in the bronchial tree during mouth breathing is then  $A_T - A_B$ . If oral deposition cannot be neglected, then the measured value would represent an upper limit for the bronchially deposited activity.

If a measure of the activity deposited in the bronchi during nasal breathing is to be obtained, a different sampler would be needed. A five 400-mesh screen-sampler, with the first screen simulating nasal cavity deposition and the other four screens simulating bronchial collection, would then provide a measure of the activity that penetrates through both the nasal cavity and the tracheobronchial region ( $A_{N+B}$ ). With the two samplers,  $A_N$  and  $A_{N+B}$ , the activity deposited in the bronchi during nasal breathing would be given by  $A_N - A_{N+B}$ . In a similar manner, a sampler to account for non-negligible oral deposition can be designed once a quantitative oral deposition relationship is available. With a 47 mm filter system that has a collection area of  $12.5 \text{ cm}^2$ , the sampling flow rate would be  $9.4 \text{ l min}^{-1}$  which is adequate to collect sufficient activity for quantitative analysis with acceptable precision.

These measurements involve compromises with respect to breathing rates. Therefore, it may still be useful to obtain more complete measurements of the activity size distributions for more complete evaluations of the deposition behavior of the progeny in the respiratory tract. However, these choices of screens and sampling face velocities do provide estimates of the activity deposited in the various regions of the respiratory tract and thus better input information for the calculation of dose. Using the concepts described in this report a variety of other screen and flow systems could be designed to meet specific other needs. This approach to the measurements represents a considerable improvement over conventional "unattached" fraction measurements since the results can be directly related to the respiratory tract deposition processes that give rise to the radiation dose to the critical tissues involved in  $^{222}\text{Rn}$ -decay product induced lung cancers.

## REVIEW AND RECOMMENDATIONS

As part of the effort to prepare this report, a workshop was convened at the University of Illinois of the leading experts from around the world to review the current state of knowledge on "unattached" fractions and the state-of-the-art in activity size measurements. This workshop was held on April 24-25, 1989 in Urbana, Illinois. The following individuals attended: Dr. E.O. Knutson (EML), Dr. K.W. Tu (EML), P. Scofield (EML), Dr. A.C. James (PNL), Dr. James Briant (PNL), Dr. Robert F. Holub (BuMines), Dr. Steven Solomon (ARL), J. Strong (NRPB), Dr. A. Reineking (Universität Göttingen), Dr. Y.S. Cheng (ITRI), and Dr. Y.F. Su (ITRI). A series of presentations were made of recent results and current activities in

developing and testing new measurement methodologies. The specific measurement results have been presented in previous sections of this report. During the final portion of the workshop, a round table discussion of a variety of issues was held.

In order to foment discussion, three general sets of issues were sent to the workshop participants before the meeting. These issues were

1. Conventional "unattached" fraction measurements.
  - a) Utility of single "unattached" fraction measurements for assessing dose.
  - b) Standardization of screen/flow parameters.
    - i) Is there a "best" choice for cut-off diameter ( $d_p(50\%)$ ) for assessing the "unattached" fraction?
    - ii) Would a measurement system based on models of respiratory deposition provide more useful estimates of the airborne activity exposure needed in dosimetric calculations?
2. Measurement of the complete activity size distribution.
  - a) Has the development of single wire mesh screen-based systems evolved to the point where reliable activity-weighted size distributions can be obtained?
    - i) Serial or Parallel Systems?
    - ii) Measurement of the activity deposited on the screen as opposed to the measurement of the activity deposited on a back-up filter?
    - iii) Choice of screen/flow values.
    - iv) Problem of collection of "attached" activity by screens providing artifact "unattached" activity.
  - b) Activity-weighted size distribution reconstruction
    - i) Twomey, Expectation Maximization, Simplex, "Micron", other?
    - ii) Error analysis
  - c) Resolution limits to the measurements.
3. Recommendations on types and timing of measurements for better exposure/dose estimation.

- a) Can we specify "typical" values for living areas and bedrooms in non-smokers and smokers households of:
  - i) Unattached fraction of potential alpha energy,  $f_p$ .
  - ii) Effective diffusional size of the "unattached" fraction.
  - iii) Activity-weighted median diameter of the "attached" fraction.
  - iv) Should explicit consideration be given to inclusion of a "nuclei" mode in the activity size distribution for the particle-attached activity in the range of 10-20 nm in diameter?
- b) Does the size distribution of "unattached" radon progeny and the particle-attached activity increase in size within the respiratory tract as a result of hygroscopic growth? If so, can "typical" growth factors be specified?

Each of these topics were discussed both in the individual presentations and in the summary discussion. It is the purpose of this section to summarize the results of these discussions and to provide specific recommendations with regards to future measurement efforts.

The "unattached" fraction is currently a quantity that is not clearly defined. Its use as a measure of highly diffusional activity is empirically defined by the measurement methods used in any particular study. However, the procedures have not been standardized and measurements based on the variety of methods discussed above are difficult to quantitatively intercompare. A standard definition of what portion of the activity-weighted size distribution is to be included in the "unattached" fraction does not currently exist. Ramamurthi and Hopke (1989) have suggested that the use of a screen system with a  $d_p(50\%)$  at 4 nm would provide an optimum collection of the smaller sizes while minimizing the collection of the nuclei mode, but this suggestion has not been adopted by the scientific community involved in radon/aerosol measurements.

A question then arises as to whether the "unattached" fraction should now be defined in terms of the amount of activity determined to be associated with particles below a certain size or continue to be operationally defined as that collected by a screen with a given  $d_p(50\%)$  value. Since the peak in the dose per unit exposure curve comes at around 4 to 5 nm, it may be that the activity less than 10 nm is the quantity most useful for dosimetry. However, given the frequency of particles in the nuclei size range of 5 to 20 nm, it would be difficult to accurately assess the less than 10 nm activity using screen collection as the separation method. Thus, it is

recommended that "unattached" fraction measurements should be made using a screen system with a  $d_p(50\%)$  of 4 to 5 nm.

In an earlier view of the deposition of the "unattached" activity and the resulting curves of dose as a function of particle size (James, 1988, for example), the curve below 10 nm is relatively flat because substantial nasal deposition was not included. However, the new information on the deposition in the nasal and oral cavities suggests that more detailed information of the activity size distribution below 10 nm is essential if the dose is to be accurately estimated. If a larger portion of the < 2 nm sized activity is deposited in the extra-thoracic region, then the conventional "unattached" fraction measurement becomes less useful in assessing risk from radon progeny and the size range around 10 nm becomes the dominant source of bronchial dose. More extensive characterization of the extra-thoracic deposition thus becomes necessary to remove a critical uncertainty in the overall exposure-dose-risk estimation.

It can be concluded from even the limited activity-weighted size distributions that have been measured that the "unattached" fraction cannot necessarily be characterized as a monodisperse mode with a single, fixed diffusion coefficient. There may be 1 or 2 modes in the size distribution below 10 nm depending on the presence of aerosol sources. In indoor spaces without sources, a classical "unattached" activity mode may exist although some measurements would suggest polydispersity in the distribution. The standard screen methods for "unattached" fraction do not perform a dichotomous separation of "attached" from "unattached" in the manner of inertial separators used in larger particle ( $> 1 \mu\text{m}$ ) applications. In some circumstances, the measurement may provide sufficient separation of the aerosol to be useful in the subsequent dosimetric calculations. Thus, the development of measurement systems that provide direct determinations of the deposited activity may provide more useful information for the estimation of dose and risk.

Complete characterization of the activity size distribution can now be accomplished with automated or manual systems. There remain uncertainties in the extraction of size distributions from the activity measurements (Ramamurthi and Hopke, 1990), and no standardization of systems is currently feasible. Further development and refinement of these systems will lead to incremental improvements in their performance and the reliability of the extracted information. There are only a limited number of such systems available. These systems are complex and expensive to build and use. They will, therefore, only have limited application in assessing the

exposure of individuals to radon progeny that will permit a relatively complete dosimetric evaluation to be made. It is likely that models will then be needed that would relate building characteristics including ventilation rates, interzonal flows, radon entry pathways, indoor aerosol sources, surface deposition, and other related phenomena to radon progeny concentrations, activity-weighted size distributions and ultimately to respiratory tract dose. Measurements of complete activity size distributions along with other related variables are needed to permit the development and verifications of phenomenological models or to validate models that would relate the radon progeny behavior to basic fluid dynamics and aerosol physics principles. Such models would then allow extrapolation of the experience gained in a reasonable number of well characterized structures to a larger population of houses in which the general public reside.

The availability of measurement methods that retain the simplicity of a screen "unattached" fraction measurement, but provide results that can be more directly related to the dosimetric calculations for which the measurements are being made would be valuable. Samplers have previously been designed to mimic the deposition of larger particles in the pulmonary region of the respiratory system. The conceptual framework for nasal and bronchial deposition samplers has been presented and appears to be an attractive alternative to "unattached" fraction measurements. However, the uncertainties in the amount of nasal deposition need to be resolved, and it is necessary that such a sampling system be built, tested, and its utility demonstrated. It is recommended that such an effort be made in the near term future. Another issue that needs to be addressed in developing a bronchial sampler is the problem of hygroscopic growth. If the particles on which the activity reside grow in size upon contact with the higher temperature and relative humidity, their aerodynamic behavior is modified and their rate of deposition is decreased. The rate of reduction in deposition and hence in the associated dose is roughly linearly related to the size. Thus, if the particles double in size, the resulting dose will be halved. There is currently no information available on the hygroscopicity of the indoor aerosol and this potential effect cannot be quantitatively evaluated. Methods are available to perform these measurements and information will become available in the next several years. Once this additional knowledge about deposition and sampler behavior is available, it may then be possible to replace "unattached" fraction as the useful measurement with the "bronchial" fraction or the "nasal" fraction.

The uncertainties in nasal and oral deposition represent major uncertainties in the evaluation of the overall risk arising from the inhalation of radon progeny. Because the dose per unit exposure from the "unattached" fraction is an order of magnitude larger than that from an equivalent amount of "attached" activity, then nasal deposition of 1 nm particles of 80 to 85% instead of 60 to 65% would result in an approximately 25% reduction in dose and particles in the range of 10 nm carrying activity would become the critical determinant of the deposited activity in the tracheobronchial region. Thus, resolution of the nasal/oral deposition question is essential in the evaluation of the importance of the "unattached" fraction in dosimetric calculations and would elevate the need for complete size distribution measurements or new samplers based on respiratory deposition in order to make accurate dose estimates.

There are currently only very limited data available on both "unattached" fractions and complete activity-weighted size distributions in indoor air. The available measurements have generally been made under artificial conditions and not in occupied houses in normal use. It may be that actual conditions will be similar to the ones that have been simulated, but additional measurements are needed to examine this question. It is therefore not currently possible to provide estimates of "unattached" fractions for which there is a high degree of confidence that they represent "typical" values in indoor air. In general it appears that the "unattached" fraction of potential alpha energy concentration measured in active working areas of uranium mines are lower than in "typical" indoor air. It appears that the "unattached" fraction values in mines are approximately 3 times smaller than those measured in houses. The more recent measurements also suggest that the equilibrium factor in houses without smokers is lower than the commonly used value of 0.5 and are probably in the order of 0.30 to 0.40. Thus, although there is less airborne activity in indoor air per unit radon activity concentration, more of it is in the more diffusive form. Now that improved understanding of the collection behavior of screens and the chemistry of radon progeny has led to improved sampling and analysis methods, these methods need to be used to provide a data base from which improved exposure-dose-risk estimates can be made.

## REFERENCES

Agarwal, J.K., G.J. Sem (1980) Continuous flow, single-particle counting condensation nuclei counter, *J. Aerosol Sci.* 11:343-358; 1980.

Bartz, H., H. Fissan, C. Helsper, Y. Kousaka, K. Okuyama, N. Fukushima, P.B. Keady, S. Kerrigan, S.A. Fruin, P.H. McMurry, D.Y.H. Pui, and M.R. Stolzenburg, (1985) Response characteristics for four different condensation nucleus counters to particles in the 3-50 nm diameter range, *J. Aerosol Sci.* 5:443-456; 1985.

Becker, K.H., A. Reineking, H.G. Scheibel, and J. Porstendörfer (1984) Radon daughter activity size distributions, *Radiat. Prot. Dosim.* 7:147-150.

BEIR IV (1988) *Health Risks of Radon and Other Internally Deposited Alpha-Emitters*, Committee on the Biological Effects of Ionizing Radiations Board on Radiation Effects Research Commission on Life Sciences, National Research Council, National Academy Press, Washington, D.C.

Bigu, J and B. Kirk, (1980) Determination of the unattached radon daughter fractions in some uranium mines, Presented at the Workshop on Attachment of Radon Daughters, Measurement Techniques and Related Topics, October 30 1980, University of Toronto, report available from CANMET, P.O. Box 100, Elliot Lake, Ontario, Canada.

Bigu, J. (1985) Radon daughter and thoron daughter deposition velocity and unattached fraction under laboratory conditions in underground uranium mines, *J. Aerosol Sci.* 16:157-165; 1985.

Blanc, D., J. Fontan, A. Chapuis, F. Billard, G. Madelaine, and J. Pradel (1968) Dosage du radon et de ses descendants dans une mine d'uranium. Repartition granulometrique des aerosols radioactifs, *Symposium on Instruments and Techniques for the Assessment of Airborne Radioactivity in Nuclear Operations*, International Atomic Energy Agency, Vienna, pp. 229-238 (1967).

Busigin, A., A.W. Van der Vooren, J.C. Babcock, and C.R. Phillips (1981a) The nature of unattached  $^{218}\text{Po}$  (RaA) particles, *Health Phys.* 40:333-343.

Busigin, A., A.W. Van der Vooren, and C.R. Phillips (1981b) Measurement of the total and radioactive aerosol size distributions in a Canadian uranium mine, *Am. Ind. Hyg. Assoc. J.* 42:310-314.

Chamberlain, A.C. and E.D. Dyson (1956) The dose to the trachea and bronchi from the decay products of radon and thoron, *Brit. J. Radiol.* 29:317-325.

Chapuis, A., A. Lopez, J. Fontan, F. Billard, and G.J. Madelaine (1970) Spectre granulometrique des aerosols radioactifs dans mine d'uranium, *J. Aerosol Sci.* 1:243-253.

Chen, R.Y. and R.A. Comparin (1976) Deposition of aerosols in the entrance of a tube, *J. Aerosol Sci.* 7:335-241.

Cheng, Y.S. and H.C. Yeh (1980) Theory of screen type diffusion battery, *J. Aerosol Sci.* 11:313-319.

Cheng, Y.S., J.A. Keating, and G.M. Kanapilly (1980) Theory and calibration of a screen-type diffusion battery, *J. Aerosol Sci.* 11:549-556.

Cheng, Y.S., Y. Yamada, H.C. Yeh, and D.L. Swift (1988) Diffusional deposition of ultrafine aerosols in a human nasal cast, *J. Aerosol Sci.* 19:741-751.

Cheng, Y.S. (1989) Deposition of thoron daughters in human head airways, Technical Exchange Meeting, Grand Junction, CO, September 18-19, 1989.

Chu, K.D. and P.K. Hopke (1988) Neutralization Kinetics for Polonium-218, *Environ. Sci. Technol.* 22:711-717.

Cohen, B.S. (1987) Deposition of Ultrafine Particles in the Human Tracheobronchial Tree: A Determinant of the Dose from Radon Daughters, in *Radon and Its Decay Products: Occurrence, Properties and Health Effects*, P.K. Hopke, ed., Symposium Series 331, American Chemical Society, Washington, D.C., pp. 475-486.

Cohen, B.S., R.G. Sussman, R.G. and M. Lippmann (1990) Ultrafine particle deposition in a human tracheobronchial cast. *Aerosol Sci. Technol.* 12: in press.

Cooper, J.A., P.O. Jackson, J.C. Langford, M.R. Petersen, and B.O. Stuart (1973) Characteristics of attached radon-222 daughters under both laboratory and field conditions with particular emphasis upon underground mine environments, Report to the U.S. Bureau of Mines under Contract H0220029 from Battelle Pacific Northwest Laboratories, Richland, WA.

Craft, B.F., J.L. Oser, and F.W. Norris, (1966) A Method for Determining Relative Amounts of Combined and Uncombined Radon Daughter Activity in Underground Uranium Mines, *Am. Ind. Hyg. Assoc. J.* 27:154-159.

Davies, C.N. (1945) Definitive equations for the fluid resistance of spheres, *Proc. Phys. Soc.* 57: 259-270.

Duggan, M.J. and D.M. Howell (1969) The Measurement of the Unattached Fraction of Airborne RaA, *Health Phys.* 17:423-427.

Egan, M.J. and W. Nixon (1989) On the relationship between experimental data for total respiratory deposition and model calculations-Part II: Application to fine particle deposition in the respiratory tract, *J. Aerosol Sci.* 20:149-156.

Emi, H., C. Kanaoka, and Y. Kuhabara (1982) The diffusion collection efficiency of fibers for aerosol over a wide range of Reynolds numbers, *J. Aerosol Sci.* 13:403-413.

EPA (1986) *A Citizen's Guide to Radon*, ODA-86-004, U.S. Environmental Protection Agency, Washington, DC.

EPA (1989) Current ORP Estimate of Annual Radon-Induced Lung Cancer Deaths in the General Population, memo dated August 17, 1989 from Margo Oge, Director, Radon Division, Office of Air and Radiation, U.S. Environmental Protection Agency, Washington, DC.

Friedlander, S.K. (1977) *Smoke, Dust and Haze*, John Wiley, Inc., New York.

Fuchs, N.A. (1964) *The Mechanics of Aerosols*, MacMillan Press, New York.

Fusamura, N., R. Kurosawa, and M. Maruyama (1967) Determination of f-value in Uranium Mine Air, *Symposium on Instruments and Techniques for the Assessment of Airborne Radioactivity in Nuclear Operations*, International Atomic Energy Agency, Vienna, pp. 213-227.

Gebhart, J., C.F. Schiller-Scotland, M.J. Egan, and W. Nixon (1989) On the relationship between experimental data for total respiratory deposition and model calculations-Part I: Effect of instrument dead space, *J. Aerosol Sci.* 20:141-147.

George A.C. (1972) Measurement of the uncombined fraction of radon daughters with wire screens, *Health Phys.* 23:390-392.

George, A.C. and A.J. Breslin (1969) Deposition of radon daughters in humans exposed to uranium mine atmospheres, *Health Phys.* 17:115-124.

George, A.C. and A.J. Breslin (1980) The Distribution of Ambient Radon and Radon Daughters in Residential Buildings in the New Jersey-New York Area, National Radiation Environment III, Vol. 2, CONF-780422. Technical Information Center, U.S. Department of Energy, p. 1272.

George, A.C. and L. Hinchliffe (1972) Measurements of Uncombined Radon Daughters in Uranium Mines, *Health Phys.* 23:791-803.

George, A.C., L. Hinchliffe, and R. Sladowski (1975) Size Distribution of Radon Daughter Particles in Uranium Mine Atmospheres, *Am. Ind. Hyg. Assoc. J.* 36:484-490.

George, A.C., L. Hinchliffe, and R. Sladowski (1977) Size Distribution of Radon Daughter Particles in Uranium Mine Atmospheres, HASL-326, Health and Safety Laboratory, New York, 9 pp.

George, A.C., M.H. Wilkening, E.O. Knutson, D. Sinclair, and L. Andrews (1984) Measurements of Radon and Radon Daughter Aerosols in Socorro, New Mexico, *Aerosol Sci. Technol.* 3:277-281.

Goldstein, S.D. and P.K. Hopke (1985) Environmental neutralization of polonium-218, *Environ. Sci. Technol.* 19:146-150.

Gormley, P. and Kennedy, M. (1949) Diffusion for a stream flowing through a cylindrical tube, *Proc. R. Irish Acad.* 52A:163-167.

Harley, N.H. and B.S. Pasternack (1982) Environmental radon daughter alpha dose factors in a five-lobed human lung, *Health Phys.* 42:789-799.

Hirst, B.W. and G.E. Harrison (1939) The diffusion of Rn gas mixtures, *Proc. Roy. Soc. Lond.* A169:573-586.

Holub, R.F. and E.O. Knutson (1987) Measuring polonium-218 diffusion-coefficient spectra using multiple wire screens, in *Radon and Its Decay Products: Occurrence, Properties and Health Effects*, P.K. Hopke, ed., Symposium Series 331, American Chemical Society, Washington D.C., pp. 340-356.

Holub, R.F., E.O. Knutson, and S. Solomon (1988) Tests of the Graded Wire Screen Technique for Measuring the Amount and Size Distribution of Unattached Radon Progeny, *Rad. Prot. Dosim.* 24:265-268.

Hopke, P.K. and M. Ramamurthi (1988) Production of Ultrafine Particles by Radon Radiolysis, *J. Aerosol Sci.* 19:1323-1325.

Hopke, P.K. (1989a) Use of Electrostatic Collection of  $^{218}\text{Po}$  for Measuring Rn, *Health Phys.* 57:39-42.

Hopke, P.K. (1989b) The Initial Behavior of  $^{218}\text{Po}$  in Indoor Air, *Environment Int.* 15:299-308.

Hopke, P.K., M. Ramamurthi and E.O. Knutson (1990) A Measurement System for Rn Decay Product Lung Deposition Based on Respiratory Models, *Health Phys.* (in press).

ICRP (1959) Report of Committee II on Permissible Dose for Internal Radiation, ICRP Publication 2, International Commission on Radiological Protection, Pergamon Press, Oxford.

ICRP (1987) *Lung Cancer Risk from Environmental Exposures to Radon Daughters*, Report of a Task Group, ICRP publication 50, International Commission on Radiological Protection, *Ann. of ICRP* 17(1).

Ingham, D.B. (1975) Diffusion of aerosols for a stream flowing through a cylindrical tube, *J. Aerosol Sci.* 6:125-132.

Jacobi, W. and K. Eisfeld (1980) Internal dosimetry of radon-222, radon-220 and their short-lived daughters, GSF report S-626, Gesellschaft für Strahlen- und Umweltforschung, Munich-Neuherberg, West Germany.

James A.C., G.F. Bradford, and D.M. Howell (1972) Collection of unattached RaA atoms using wire gauze, *J. Aerosol Sci.* 3:243-254.

James, A.C., J.R. Greenhalgh, and A. Birchall (1980) A Dosimetric Model for Tissues of the Human Respiratory Tract at Risk from Inhaled Radon and Thoron Daughters, in *Radiological Protection - Advances in Theory and Practice*, Proc. 5th Congress IRPA, Jerusalem, March 1980. Volume 2, Pergamon Press, Oxford, 1045-1048.

James, A.C. (1984) Dosimetric approaches to risk assessment for indoor exposure to radon daughters, *Rad. Prot. Dosim.* 7:353-366.

James, A.C. (1988) Lung dosimetry, In: *Radon and its Decay Products in Indoor Air*, Nazaroff W.W. and A.V. Nero, eds., Wiley-Interscience, New York, pp. 259-309.

James, A.C., R.C. Roth, R.W. Kuennen, and F.T. Cross (1989) The efficacy of a high efficiency room air treatment system in mitigating dose from radon decay products, presented at American Association of Aerosol Research meeting, Reno, NV.

Jonassen, N. (1984) Electrical Properties of Radon Daughters, presented at the International Conference on Occupational Radiation Safety in Mining, Toronto, Canada.

Jonassen, N. and J.P. McLaughlin (1985) The Reduction of Indoor Air Concentrations of Radon Daughters without the Use of Ventilation, *Sci. Total Environ.* 45:485-492.

Khan, A., C.R. Phillips, and P. Duport (1987) Analysis of errors in the measurement of unattached fractions of radon and thoron progeny in a Canadian uranium mine using wire screen methods, *Rad. Prot. Dosim.* 18:197-208.

Knutson, E.O., A.C. George, R.H. Knuth, and B.R. Koh (1984) Measurements of radon daughter particle size, *Radiat. Prot. Dosim.* 7:121-125.

Knutson, E.O., K.W. Tu, S.B. Solomon, and J. Strong (1988) Intercomparison of three diffusion batteries for the measurement of radon decay product particle size distributions, *Radiat. Prot. Dosim.* 24:261-264.

Kojima, H. and S. Abe (1988) Measurement of the total and unattached radon daughters in a house, *Radiat. Prot. Dosim.* 24:241-244.

Kotrappa, P. and Y.S. Mayya (1976) Revision of Raghavayya and Jones' Data on the Radon Decay in Mine Air, *Health Phys.* 31:380-382.

Kulju, L.M., M. Ramamurthi, and P.K. Hopke (1986) The detection and measurement of the activity size distribution of ultrafine particles, Paper No. 86-40.6, Air Pollution Control Association, Pittsburgh, PA.

Liu, B.Y.H. and D.Y.H. Pui (1975) On the performance of the electrical aerosol analyzer, *J. Aerosol Sci.* 6:249-264.

Lodge, Jr., J.P. and T. Chan (1986) *Cascade Impactor: Sampling & Data Analysis*, American Industrial Hygiene Association, Akron, OH, 170 pp.

Loeb, L.B. (1961) *The Kinetic Theory of Gases*, 3rd Ed., Dover Publications, New York.

Maher, E.F. and N.M. Laird (1985) Algorithm reconstruction of particle size distribution from diffusion battery data, *J. Aerosol Sci.* 16:557-570.

Mercer, T.T. and W.A. Stowe (1969) Deposition of unattached radon decay products in an impactor stage, *Health Phys.* 17:259-264.

Mercer, T.T. (1975) Unattached radon decay products in mine air, *Health Phys.* 28:158-161.

NCRP (1984) *Exposure from the Uranium Series with Emphasis on Radon and Its Daughters*, NCRP Report No. 77, National Council on Radiation Protection and Measurements, Bethesda, MD.

Porstendorfer, J. (1968) Die diffusionkoeffizienten und mittleren freien weglangen der geladenen und neutral radon-folge produkte in luft, *Z. Physik* 213:384-396.

Porstendorfer, J. and T.T. Mercer (1979) Influence of electric charge and humidity upon the diffusion coefficient of radon decay products, *Health Phys.* 15:191-199.

Porstendorfer, J., G. Röbig, and A. Ahmed (1979) Experimental determination of the attachment coefficients of atoms and ions on monodisperse particles, *J. Aerosol Sci.* 10:21-28.

Porstendorfer, J. (1987) Free-fractions, attachment rates, and plate-out rates of radon daughters in houses, in *Radon and Its Decay Products: Occurrence, Properties and Health Effects*, P.K. Hopke, ed., Symposium Series 331, American Chemical Society, Washington, D.C., pp. 285-300.

Raabe, O.G. (1969) Concerning the interactions that occur between radon decay products and aerosols, *Health Phys.* 17:177-185.

Raes, F., A. Janssens, A. DeClercq, and H. Vanmarcke (1984) Investigation of the indoor aerosol and its effect on the attachment of radon daughters, *Rad. Prot. Dosim.* 7:127-131.

Raes, F. (1985) Description of properties of unattached  $^{218}\text{Po}$  and  $^{212}\text{Pb}$  particles by means of the classical theory of cluster formation, *Health Phys.* 49:1171-1187.

Raghavayya, M. and J.H. Jones (1974) A wire screen-filter paper combination for the measurement of fractions of unattached daughter atoms in uranium mines, *Health Phys.* 26:417-430.

Ramamurthi, M. and P.K. Hopke (1989) On improving the validity of wire screen "unattached" fraction Rn daughter measurements, *Health Phys.* 56:189-194.

Ramamurthi, M., P.K. Hopke, R. Strydom, K.W. Tu, E.O. Knutson, R.F. Holub, W. Winklmayr, W. Marlow and S.C. Yoon (1989) Radon Decay Product Activity Size Distribution Measurement Methods - A Laboratory Intercomparison, presented at the American Association for Aerosol Research, Reno, NV. October 1989.

Ramamurthi, M. and P.K. Hopke (1990a) An Automated, Semi-Continuous System for Measuring Indoor Radon Progeny Activity-Weighted Size Distributions,  $d_p$ : 0.5-500 nm, *Aerosol Sci. Technol.* (paper under review).

Ramamurthi, M. and P.K. Hopke (1990b) Simulation studies of reconstruction algorithms for the determination of optimum operating parameters and resolution of graded screen array systems (non-conventional diffusion batteries), *Aerosol Sci. Technol.* (in, press).

Ramamurthi, M., R. Strydom, and P.K. Hopke (1990a) Assessment of wire and tube penetration theories using a  $^{218}\text{PoO}_x$  cluster aerosol, *J. Aerosol Sci.* (in press).

Ramamurthi, M., R. Strydom, P.K. Hopke, and R.F. Holub, (1990b) Formation of ultrafine aerosols from radon radiolysis under laboratory conditions. *J. Aerosol Sci.* Submitted for review; April 1990.

Reineking, A., K.H. Becker, and J. Porstendörfer (1985) Measurements of the unattached fractions of radon daughters in houses, *Sci. Total Environ.* 45:261-270.

Reineking, A. and J. Porstendörfer (1986) High-volume screen diffusion batteries and  $\alpha$ -spectroscopy for measurement of the radon daughter activity size distributions in the environment, *J. Aerosol Sci.* 17:873-879.

Reineking, A., K.H. Becker, and J. Porstendörfer (1988) Measurement of activity size distributions of the short-lived radon daughters in the indoor and outdoor environment, *Radiat. Prot. Dosim.* 24:245-250.

Reineking, A. and J. Porstendörfer (1990) The unattached fraction of the short-lived radon decay products in the indoor and outdoor environment, *Health Phys.* (in press).

Scheibel, H.G. and J. Porstendörfer (1984) Penetration measurements for tube and screen type diffusion batteries in the ultrafine particle size range, *J. Aerosol Sci.* 15:673-682.

Schiller, C. (1985) *Diffusionabscheidung von Aerosolteilchen im Atemtrakt des Menschen*, Ph.D. thesis, J.W. Goethe Universität, Frankfurt/Main, West Germany.

Shimo, M. and Y. Ikebe (1984) Measurements of radon and its short-lived decay products and unattached fraction in air, *Rad. Prot. Dosim.* 8:209-214.

Shimo, M., Y. Yoshihiro, K. Hayashi, and Y. Ikebe (1985) On some properties of  $^{222}\text{Rn}$  short-lived decay products in air, *Health Phys.* 48:75-86.

Sinclair, D., A.C. George, and E.O. Knutson (1977) Application of diffusion batteries to measurement of submicron radioactive aerosols, in *Airborne Radioactivity*, American Nuclear Society, La Grange Park, IL, 103-114.

Stranden, E. and L. Berteig (1982) Radon daughter equilibrium and unattached fraction in mine atmospheres, *Health Phys.* 42:479-487.

Stranden, E. and T. Strand (1986) A dosimetric discussion based on measurements of radon daughter equilibrium and unattached fraction in different atmospheres, in *Radiation Protection Dosimetry*. 16:313-318.

Strong, J.C. (1988) The size of attached and unattached radon daughters in room air, *J. Aerosol Sci.* 19:1327-1330.

Strong, J.C. (1989) Design of the NRPB activity size measurement system and results, presented at the Workshop on "Unattached" Fraction Measurements, University of Illinois, Urbana, IL, April 1989.

Subba Ramu, M.C. (1980) Calibration of a diffusion sampler used for the measurement of unattached radon daughter products, *Atmospheric Environ.* 14:145-147.

Tan, C.W. (1969) Diffusion of disintegration products of inert gases in cylindrical tubes, *Int. J. Heat Mass Trans.* 12:471-478.

Task Group on Lung Dynamics (1966) Deposition and retention models for internal dosimetry of the human respiratory tract, *Health Phys.* 29:673-680.

Thomas, J.W. (1955) The diffusion battery method for aerosol particle size determination, *J. Colloid Sci.* 10:246-255.

Thomas, J.W. (1970) Modification of the Tsivoglou method for radon daughters in air, *Health Phys.* 19:691-693.

Thomas J.W. and L.E. Hinchliffe (1972) Filtration of 0.001  $\mu\text{m}$  particles with wire screens, *J. Aerosol Sci.* 3:387-393.

Tu, K.W and E.O. Knutson (1988a) Indoor radon progeny particle size distribution measurements made with two different methods, *Rad. Prot. Dosim.* 24:251-255.

Tu, K.W and E.O. Knutson (1988b) Indoor outdoor aerosol measurements for two residential buildings in New Jersey, *Aerosol Sci. Technol.* 9:71-82.

Tu, K.W., A.C. George. and Knutson, E.O. (1989) Summary of results of radon progeny particle size in indoor air, presented to the American Association for Aerosol Research, Reno, NV, Oct. 1989; and personal communications.

Twomey, S. (1975) Comparison of constrained linear inversion and an iterative nonlinear algorithm applied to the indirect estimation of the particle size distribution, *J. Comp. Phys.* 18:188-200.

Van der Vooren, A.W., A. Busigin, and C.R. Phillips (1982) An evaluation of unattached radon (and thoron) daughter measurement techniques, *Health Phys.* 42:801-808.

Vanmarcke, H., A. Janssens, and F. Raes (1985) The equilibrium of attached and unattached radon daughters in the domestic environment, *Sci Tot. Environ.* 45:251-260.

Vanmarcke, H., A. Janssens, F. Raes, A. Poffijn, P. Perkvens, and R. Van Dingenen (1987) The behavior of radon daughters in the domestic environment, in *Radon and Its Decay Products:*

*Occurrence, Properties and Health Effects*, P.K. Hopke, ed., Symposium Series 331, American Chemical Society, Washington, D.C., pp. 301-323.

Vanmarcke, H., A. Reineking, J. Porstendorfer, and F. Raes (1988) Comparison of two methods for investigating indoor radon daughters, *Rad. Prot. Dosim.* 24:281-284.

Vanmarcke, H., P. Berkvens, and A. Poffijn (1989) Radon versus Rn daughters, *Health Phys.* 56: 229-231.

Yeh, H.C., Y.S. Cheng, and M.M. Orman (1982) Evaluation of various types of wire screens as diffusion battery cells, *J. Colloid Interface Sci.* 86:12-16.

Yeh, H.C. and G.M. Schum (1980) Models of human airways and their application to inhaled particle deposition, *Bull. Math. Biol.* 42:461-480.

Yu, C.P., C.K. Diu, and T.T. Soong (1981) Statistical analysis of aerosol deposition in nose and mouth, *Am. Ind. Hyg. Assoc. J.* 42:726-733.

Yu, C.P. and C.K. Diu (1982) A comparative study of aerosol deposition in different lung models, *Am. Ind. Hyg. Assoc. J.* 42:54-65.